From Causal Discovery to Intervention Simulation: Modeling Precarity and Depression in the HELIUS Study

Kyuri Park[1], Leonie K. Elsenburg[2], Mary Nicolao[2], Karien Stronks[2], Vítor V. Vasconcelos[1, 3]

[1] *Computational Science Lab, Informatics Institute, University of Amsterdam, PO Box 94323, Amsterdam, 1090GH, the Netherlands*
[2] *Department of Public and Occupational Health, Amsterdam Public Health Research Institute, Amsterdam UMC, University of Amsterdam, Amsterdam, the Netherland*
[3] *Institute for Advanced Study, University of Amsterdam, Oude Turfmarkt 147, Amsterdam, 1012GC, the Netherland*

2025-05-14

Abstract

This study investigates the dynamic relationship between precarious life conditions and depression by combining constraint-based causal discovery with computational modeling. Using cross-sectional data from the HELIUS study, we applied cycle-capable causal discovery algorithms to uncover directional relationships between financial stress, domain-specific precariousness indicators, and depressive symptoms. Our multi-resolution analysis—spanning both aggregate and symptom-level constructs—identified financial stress as a robust driver of depression, and highlighted key symptoms, such as sleep disturbance and depressed mood, as likely initiators or reinforcers of downstream precariousness. To explore how these structural insights shape intervention effectiveness, we developed a simplified nonlinear dynamical model simulating the co-evolution of depression and social precarity under varying levels of financial stress reduction. Simulation results revealed that the system's responsiveness depends not only on the intensity of external intervention but also on internal structural features such as feedback strength and noise. In particular, some configurations exhibited bistability, requiring interventions to surpass a critical threshold to trigger lasting improvement, while others responded more proportionally. Together, these findings emphasize that internal feedback dynamics—not just external adversity—can shape the impact of mental health interventions. More broadly, our study offers a scalable framework for integrating causal discovery and dynamical simulation to better understand and inform policy responses to complex psychosocial phenomena.

Table of contents

1 Introduction

Mental health disorders represent a growing global health concern, especially in urbanized regions (Gruebner et al., 2017; World Health Organization, 2022). In 2019, one in eight people worldwide were living with a mental health condition, with the highest disability-adjusted life years (DALYs) due to mental and addictive disorders concentrated in high-income countries such as those in Northern Europe, North America, and Australia (Rehm & Shield, 2019; World Health Organization, 2022). Despite growing awareness, governments have struggled to design effective responses. Mental health outcomes arise from complex, multi-level dynamics—intertwined with the social, economic, and spatial structures of urban environments—making both diagnosis and intervention design deeply challenging (Van Der Wal et al., 2021).

Recent work has shifted focus from individual-level vulnerability to broader social and structural determinants. While high-income nations show elevated overall DALYs, within-country disparities reveal that income inequality is a significant predictor of mental health burden (Rehm & Shield, 2019). Moreover, precarious working conditions, housing instability, and neighborhood disadvantage have all been linked to increased risk of depression and anxiety (Fone et al., 2014; Pevalin et al., 2017; Rönnblad et al., 2019; Rugulies et al., 2023). This growing literature highlights that poor mental health is not merely a personal issue, but one rooted in sustained socioeconomic stress and structural uncertainty.

Building on this, recent studies have introduced the concept of precariousness as a multidimensional condition characterized by instability and lack of control across several life domains—including employment, finances, housing, social relations, and cultural belonging (Elsenburg et al., 2025). This broader view reveals how different forms of insecurity can co-occur and compound, forming an ecosystem of risk. However, despite growing evidence of association between precariousness and mental health, a fundamental question remains unresolved: *How do these factors causally influence one another?* Most existing studies rely on cross-sectional correlations, leaving open questions about directionality and feedback. Without stronger causal insight, it remains difficult to identify priority targets for intervention or to anticipate unintended effects.

This study aims to investigate the causal mechanisms linking precariousness and depression—and how those mechanisms shape system responses to external intervention. Specifically, we ask: *How does the internal configuration of* *the precarity–depression relationship affect the outcomes of stress-reducing interventions?* To answer this, we combine two approaches. First, we use cycle-capable causal discovery algorithms to infer directional relationships among financial stress, domain-specific precariousness factors, and depressive symptoms. By analyzing both aggregate scores (e.g., PHQ-9 total, composite precarity index) and disaggregated variables (individual symptoms and life-domain indicators), we identify both broad associations and fine-grained causal pathways. Second, we translate these insights into a computational dynamical model that simulates how depression and precarity co-evolve under varying levels of external stress. This model enables us to probe how system properties—such as feedback strength and stochastic noise—govern responsiveness to intervention. In some configurations, the system exhibits bistability, remaining stuck in a high-risk state unless external support exceeds a critical threshold. In others, it shows unistable behavior, responding more gradually to incremental changes. By integrating causal discovery with dynamic simulation, we aim to demonstrate how the internal structure of the depression–precarity system shapes its susceptibility to change—and, by extension, how intervention strategies might be tailored to the architecture of underlying vulnerability.

2 Methods

2.1 Data

We use data from the HELIUS (HEalthy LIfe in an Urban Setting) study, which has been described in detail elsewhere (Snijder et al., 2017; Stronks et al., 2013). It captures the diverse population of the city of Amsterdam by including the six main ethnic groups and which provides comprehensive health and lifestyle data, including depressive symptoms as measured by the PHQ-9 (Galenkamp et al., 2017). To operationalize indicators of precariousness, we draw on the framework outlined in previous research (Elsenburg et al., 2025) and select a set of relevant variables. To ensure a robust representation of precariousness in our causal discovery models, we conducted various exploratory analyses to identify consistent and meaningful data-driven factor structures. Based on these analyses, we identified five precariousness factors, including two related to recent stressors, each comprising multiple variables as outlined below. DFurther details on the HELIUS study and factor extraction are provided in the Appendix.

- Employment precariousness: `emp_stat`, `work_sit`.
- Social precariousness: `soc_freq`, `soc_adq`.
- Housing precariousness: `nb_safe`, `nb_res`, `nb_rent`, `cul_rec`.
- Recent relational stressors: `frd_brk12`, `conf12`.
- Recent financial stressors: `fincri12`, `inc_diff`.

After preprocessing, the HELIUS dataset comprises 21,628 samples. Along with the five precariousness factors, we also compute an overall precarity score as the combined value of these factors. Additionally, PHQ-9 scores are included to represent depression, both as a total sum score and as individual symptom scores. In the subsequent causal discovery analysis, we examine the relationship between depression and precarity using both aggregated sum scores and their individual-level representations. Refer to Figure 1 for the overall distributions of the variables used in the analysis.

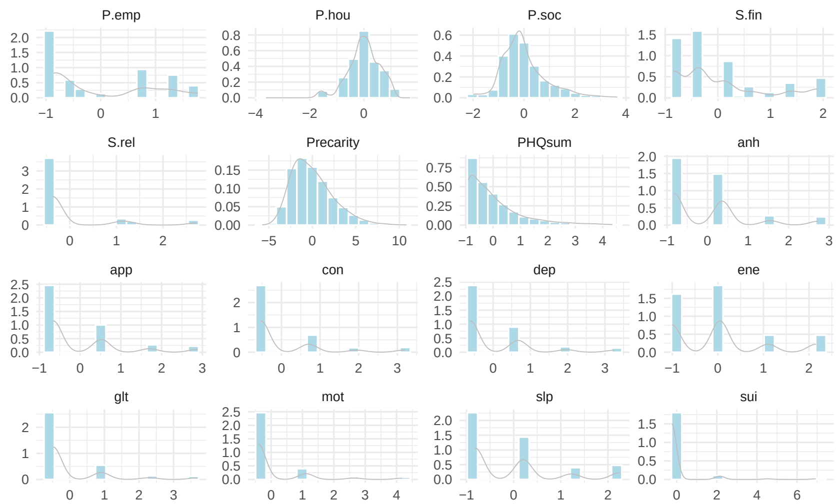

Figure 1: Distributions of variables with density overlay.
P.emp = employment precariousness; *P.hou* = housing precariousness; *P.soc* = social precariousness; *S.fin* = recent financial stressors; *S.rel* = recent relational stressors; *Precarity* = overall precarity; *PHQsum* = PHQ-9 sum score; *anh* = anhedonia; *app* = appetite; *con* = concentration; *dep* = depressed mood; *ene* = energy; *glt* = guilty; *mot* = motor; *sui* = suicidal

2.2 Causal Discovery

To uncover directional relationships between precariousness and depression, we used constraint-based causal discovery algorithms that allow for feedback loops and latent confounding. Specifically, we applied the *Fast Causal Inference* (FCI) and *Cyclic Causal Inference* (CCI) algorithms, both of which can detect cycles and non-acyclic structures (Mooij & Claassen, 2020; Strobl, 2019). For reference, we also included the *PC* algorithm, one of the most widely used methods for acyclic causal discovery (Spirtes et al., 2001).

A key challenge in applying these algorithms to the HELIUS dataset is that many variables are non-Gaussian and their relationships are likely nonlinear. To address this, we supplemented the commonly used Gaussian conditional independence (CI) test—based on partial correlations—with a non-parametric alternative: the *Randomized Conditional Correlation Test* (RCoT). RCoT approximates kernel-based CI testing using random Fourier features, significantly reducing computational demands while maintaining sensitivity to nonlinear dependencies (Strobl et al., 2019; Zhang et al., 2012).

We examined the causal structure using three complementary approaches:

1. Aggregate-level analysis: relationships between five domain-specific precariousness factors and the PHQ-9 sum score.
2. Fully disaggregated analysis: relationships between individual precariousness items and individual depressive symptoms.
3. Mixed analysis: relationships between individual symptoms and a composite index of overall precariousness.

The aggregate analysis reduces dimensionality and yields interpretable summaries of how domains of precarity relate to overall depression severity. However, it may obscure finer-grained effects. The disaggregated analysis allows for precise mapping of which symptoms are influenced by (or influence) specific precariousness conditions, but it introduces complexity due to the high dimensionality and distributional properties of the data. The mixed approach, in turn, integrates these perspectives by examining how individual symptoms respond to cumulative precarity across domains.

To ensure robust estimation and guard against sensitivity to parameter settings, we implemented a systematic grid of analysis conditions:

- Significance levels: α = 0.01 and 0.05
- Bootstrap thresholds: 0.5, 0.6, 0.7, 0.8
- CI tests: Gaussian and RCoT
- Algorithms: FCI, CCI, and PC

Each combination was bootstrapped 100 times for sum-score level analyses and 30 times for symptom-level analyses, yielding a total of 1,600 graphs per algorithm for the full analysis. For symptom networks, we fixed the skeleton structure using a consensus graph estimated across PC, FCI, and CCI (α = 0.01, RCoT). This constraint improves computational efficiency without limiting the estimation of directional edges between symptoms and precariousness variables.

To summarize the results, we adopted a two-level aggregation strategy. First, within each analysis condition, we recorded the most frequently observed edge-endpoint type (e.g., directed, undirected, uncertain) from the bootstraps. Then, across all conditions, we tallied the most frequent endpoint type per edge. In cases of ties, we assigned dashed edges to reflect uncertainty. For transparency, we accompany each graph with a table showing the relative frequencies of each edge symbol.

This procedure yields a final graph for each algorithm and analysis type—offering both robustness and interpretability. See Figure 2 for an overview of the causal discovery pipeline.

For detailed explanations of the algorithms, edge interpretations, and graph types (e.g., PAG, MAAG, CPDAG), as well as algorithmic assumptions and limitations, see the Appendix.

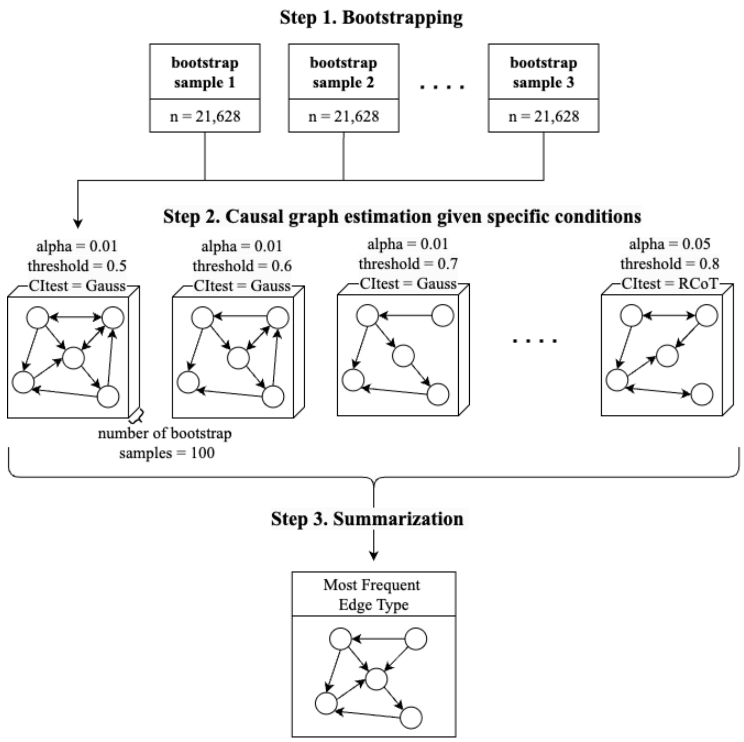

Figure 2: Analysis workflow applied across all three algorithms.

2.3 Modeling Dynamics between Precarity and Depression

To explore how internal system structure shapes responses to external support, we implement a high-level computational model that formalizes key mechanisms suggested by the causal discovery analysis. Rather than attempting to replicate the full estimated causal graph, this model abstracts the essential structure into a compact, tractable system focused on dynamic interactions between depression and social precariousness, both influenced by financial stress.

As illustrated in Figure 3, the model includes three components: depression (D), represented by the PHQ-9 sum score, social precariousness (P), and external financial stress (S). Depression and precariousness are modeled as coupled state variables that influence each other over time, with S acting as a shared input. These dynamics are formalized as a pair of nonlinear stochastic differential equations (SDEs):

$$dP = \lambda_P \left(\tanh(\alpha_1 S + \alpha_2 D) - P\right) dt + \sigma_1 dW_1$$
$$dD = \lambda_D \left(\tanh(\beta_1 S + \beta_2 P) - D\right) dt + \sigma_2 dW_2$$

Here, D denotes depression, P denotes social precariousness, and S is the external stressor associated with financial stress. The parameters λ_D and λ_P control the timescales over which variable adjusts toward its input-driven target state. The coefficients α_1, α_2 and β_1, β_2 represent the strengths of the causal influences between variables. Stochastic fluctuations are introduced through the terms $\sigma_1 dW_1$ and $\sigma_2 dW_2$, where dW_1 and dW_2 are independent Wiener processes. The system uses the hyperbolic tangent function ($tanh$) to bound the influence of inputs, ensuring smooth, saturating dynamics and preventing runaway feedback loops. Importantly, the nonlinearity introduced by the $tanh$ function also allows the system to exhibit bistability, supporting the existence of two stable states: one corresponding to low depression and precariousness, and the other to high depression and precariousness.

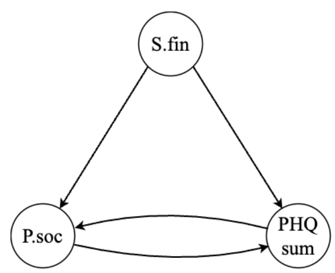

Figure 3: Conceptual high-level causal structure of precariousness and depression system.

2.3.1 Model Calibration

To identify realistic parameter settings for the simulation model, we calibrated six free parameters—α_1, α_2, β_1, β_2, and noise amplitudes σ_1, σ_2—using the Non-dominated Sorting Genetic Algorithm II (NSGA-II) (Deb et al., 2002), a multi-objective evolutionary optimization method well-suited for noisy and high-dimensional search spaces. The goal was to match simulated system behavior to empirical summary statistics derived from the HELIUS dataset, including the means and variances of depression (D) and social precariousness (P), as well as their partial correlations after adjusting for financial stress (S), specifically $\rho_{DP.S}$, $\rho_{DS.P}$, and $\rho_{PS.D}$. Given the stochastic nature of the model, each candidate parameter set was evaluated by simulating 1,000 independent trajectories, each representing an individual with a fixed S value sampled from the observed distribution. Final-state values were extracted and aggregated to compute population-level summary statistics. Fitness was assessed as the absolute deviation from the empirical targets, aggregated across all objectives. NSGA-II was implemented via the nsga2R package (Franz & Nakamura, 2015), with a population of 300 evolved over 300 generations using standard hyperparameters (crossover probability = 0.9, mutation probability = 0.25, and tournament size = 2). This process yielded a diverse ensemble of Pareto-efficient solutions balancing trade-offs between objectives. From the resulting Pareto front (Figure 4), we selected the top 30 parameter sets with the lowest combined error to use in the subsequent simulations assessing intervention effects.

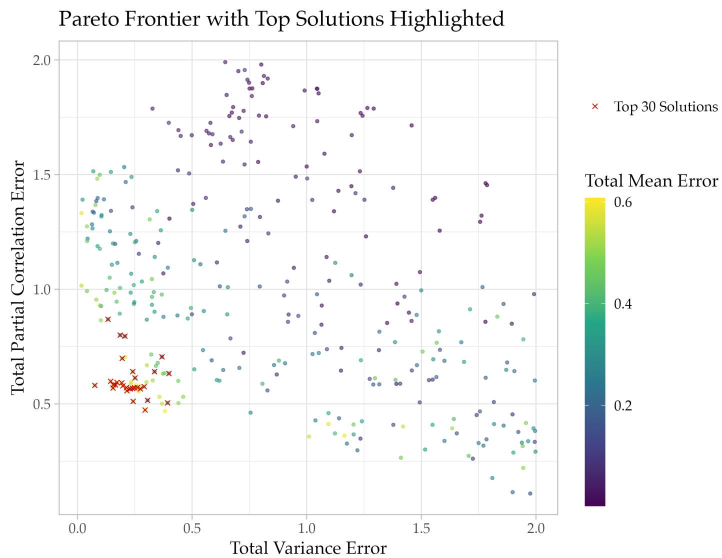

Figure 4: Pareto front of simulated parameter sets. *Each point represents a solution evaluated by its total variance error (x-axis) and total partial correlation error (y-axis), with color indicating total mean error. Red crosses highlight the top 30 solutions used for simulation.*

2.3.2 Intervention Simulation

To evaluate the effects of hypothetical support, we simulate scenarios in which each individual's financial stress level (S) is proportionally reduced toward the minimum observed value. This models a population-wide intervention applied at varying strengths — from no reduction in stress (0%) to complete alignment with the minimum observed stress level (100%).

For each of the top 30 calibrated parameter sets, we simulate the system's evolution across 300 individuals under a continuum of intervention levels. Each simulation run generates final values for D and P, which are then used to assess how internal model parameters influence the system's behavior under changing external conditions.

3 Results

3.1 Causal Structure Linking Precarity and Depression

3.1.1 Depression as sum score

The sum score graphs provide a high-level summary of how precarity factors collectively influence overall depression severity, focusing on aggregated relationships. Figure 5 illustrates the causal relationships between precariousness factors (*P.hou*, *P.emp*, *P.soc*, *S.rel*, *S.fin*) and the depression sum score (*PHQsum*), as identified by the FCI algorithm. As described in Section 2.2, dashed edges indicate ties, with the exact edge endpoint where the tie occurs is represented by a bold horizontal bar.

The causal graph in panel (a) highlights key pathways in the relationships between precarity factors and depression (PHQsum). Employment precarity (P.emp) and social precarity (P.soc) are not identified as causes of depression, whereas financial stress (S.fin) appears to play a causal role. While P.emp and P.soc are generally not recognized as causes of other precariousness factors, S.fin emerges as a potential cause, as indicated by its circle edge endpoint. Supporting this, the proportion matrix plot in panel (b) shows that S.fin has some probability of causally influencing either P.emp or P.soc.

The matrix plot can be interpreted such that the symbol in matrix[i, j] represents the relationship $i - [symbol]\ j$. For example, if matrix[i, j] is > and matrix[j, i] is $\circ$, then the inferred relationship is $i \circ\!\!\rightarrow j$. In the table, different edge types are represented by distinct colors: light gray for the absence of an edge, blue for circles, green for arrowheads, and coral for arrowtails. The colors are blended based on the proportion of each edge type, with higher proportions increasing the opacity of the corresponding color, making dominant symbols more visually prominent.

Relational stress (S.rel) plays a more nuanced role, interacting with depression and S.fin through a latent confounder. Its relationship with P.soc remains less certain, as the proportion table suggests a fair probability that this connection is absent, uncertain, or bidirectional. Meanwhile, housing precarity (P.hou) is not directly causally related to depression but is linked to P.emp and S.fin. While P.emp and S.fin are identified as non-causes of P.hou, it remains unclear whether P.hou causally influences P.emp or if their relationship is mediated by an unobserved confounder.

The findings from the CCI algorithm (see Figure 10) are largely consistent with those from the FCI algorithm, with one exception: CCI does not identify S.fin as a cause of depression. Additionally, CCI introduces greater uncertainty in edge directions, with more ties mainly between circle and arrowhead endpoints, and tends to favor arrowheads more frequently than FCI. Despite these differences, the skeleton structure and overall causal directions derived from CCI align well with the results of the FCI algorithm, supporting the key pathways.

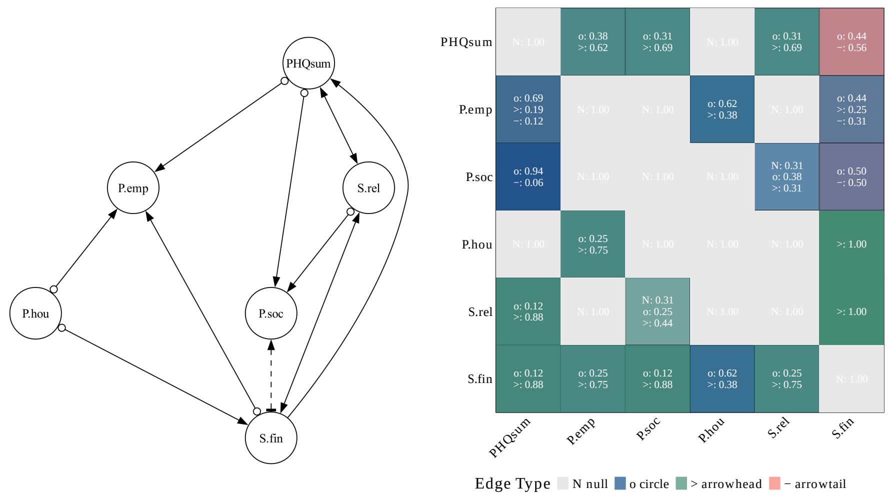

(a) FCI PAG

(b) Proportion matrix

Figure 5: Resulting graph of precarity factors and depression sum score using FCI and proportion of edge endpoint types.

3.1.2 Individual depression symptom

Moving from the sum score representation to the disaggregated symptom-level graph provides a more granular perspective on the causal relationships between precariousness factors and depression symptoms. Unlike the sum score graph, which aggregates all symptoms into a single measure—potentially obscuring nuanced relationships—the symptom-level graph highlights heterogeneity in how precariousness factors influence individual depressive symptoms: con (concentration), slp (sleep), ene (energy), app (appetite), mot (motor), sui (suicidal), anh (anhedonia), glt (guilt), and dep (depressed mood), and vice versa.

The symptom-level graph in Figure 6 panel (a) reveals a more complex and interconnected structure than the sum score graph, reflecting the strong interdependence among symptoms and suggesting much presence of latent confounders, as indicated by numerous bidirectional edges. As before, dashed edges denote ties, with specific ties marked by bold horizontal bars. In Figure 6 panel (b), the proportion matrix provides more insight into these directionalities. Here, opaque green dominates most symptom-to-symptom connections, indicating that arrowheads are the most frequently inferred edge type. However, blue regions, which correspond to circle endpoints, are particularly common for anh, slp, ene, and sui, reflecting uncertainty in the causal direction among these symptoms. Notably, the only arrowtail connection appears between dep and anh, suggesting that anhedonia (anh) is a potential cause of depressed mood (dep).

Looking at the symptom-precariousness connections, one of the key patterns is that ties are most frequently found in the relationships between individual symptoms and precariousness factors. This suggests that these causal links may be less stable across different conditions. Upon closer examination, most ties arise due to discrepancies between the Gaussian CI test and the RCoT test—with Gaussian CI favoring arrowheads and RCoT more often predicting the absence of an edge.

This discrepancy likely arises from a combination of factors. First, as the analysis shifts from aggregated to disaggregated variables, the number of conditional independence (CI) tests increases, leading to a loss of statistical power in high-dimensional causal discovery. With more variables being conditioned on, the data becomes sparser, making it harder to detect weaker dependencies. Additionally, over-conditioning—controlling for too many variables—can artificially remove statistical associations, leading to false negatives. Beyond this general statistical power issue, the fundamental differences in how these CI tests operate contribute to the inconsistency. RCoT, as a nonparametric test, does not assume linearity and can capture both linear and nonlinear dependencies. However, it is more conservative and requires larger sample sizes, making it more prone to false negatives in high-dimensional settings. In contrast, partial correlation (Gaussian CI test) assumes linear Gaussian relationships, making it more permissive and sometimes detecting weak dependencies that may not be statistically meaningful. As a result, when Gaussian CI detects an edge while RCoT does not, it could indicate that the relationship is weak, strictly linear, or requires more data for reliable nonparametric detection. This explains why many ties in the proportion matrix show a 50-50 split between symbols—where half of the conditions with RCoT suggest the absence of an edge, while the other half using Gaussian CI test favor an arrowhead. This systematic divergence highlights the challenges of causal discovery in high-dimensional settings, where varying statistical assumptions can lead to differing conclusions about the presence and direction of causal relationships.

Despite these differences, some consistent patterns emerge across both CI tests, particularly in the case of financial stress (S.fin), which appears to be connected to nearly all other variables—though many of these connections are marked by ties, reflecting uncertainty in directionality. One exception is the stronger evidence suggesting that S.fin may cause changes in app (appetite), while its relationships with other symptoms, such as ene, mot, and dep, remain ambiguous. Similarly, social precarity (P.soc) exhibits numerous connections with depressive symptoms, with most edges pointing toward P.soc rather than outward from it. This suggests that depressive symptoms, particularly dep and glt, may contribute to worsening social precarity rather than the other way around. Additionally, anh also shows some probability of causally influencing P.soc, reinforcing the idea that social precarity is more often a consequence rather than a driver of depressive symptoms.

Other precariousness factors exhibit more uncertain but still notable relationships. Relational stress (S.rel) shows weak but existing connections with slp, glt, and app, though directionality remains unclear in many cases. Employment precarity (P.emp) also connects to symptoms like slp, mot, and con, but, like S.rel, these relationships exhibit a 50/50 split in directionality, reflecting uncertainty in the inferred causal paths. In line with the aggregated graph in Figure 5, housing precarity (P.hou) does not appear to have any direct relationship with depression symptoms but consistently shows associations with employment precarity (P.emp) and financial stress (S.fin). The causal relationships among precariousness factors remain largely unchanged from the aggregated analysis, with financial stress (S.fin) exhibiting the strongest tendency to influence other precariousness factors.

Among depressive symptoms, dep, glt, and slp appear to be the most connected to precariousness factors, while P.soc has the most connections with symptoms, predominantly as a recipient rather than a driver of influence. Within the symptom network, slp, sui, and anh emerge as causally influential symptoms, as they exhibit more outgoing arrows compared to other symptoms. On the other hand, con, mot, dep, and glt, despite having high connectivity, predominantly receive incoming arrows, indicating they are more likely effects rather than causes. Considering both symptom-precariousness connections and symptom-level dynamics, sleep disturbance (slp) emerges as a central symptom, given its strong ties to precariousness factors and its influential role within the symptom network. This suggests that sleep issues could be an initiating symptom, particularly sensitive to relational stress and employment precarity. On the other hand, social precarity (P.soc) serves as a key bridge between the depression and precariousness subsystems, as depressive symptoms appear to feed back into social precarity, reinforcing a self-sustaining dynamic between depression and precarious conditions.

Finally, the results from CCI are largely consistent with those from FCI, but with some key differences. CCI tends to favor arrowheads more frequently, resulting in a greater number of bidirectional edges, which suggests a higher involvement of latent confounders. Additionally, CCI exhibits more tie situations, though, similar to FCI, most ties occur between absence and arrowhead edges, reflecting the discrepancy between the Gaussian CI test and RCoT—where the Gaussian test favors arrowheads, while RCoT more often suggests the absence of an edge. For a detailed visualization of the CCI-derived graph and proportion matrix, see Figure 11.

3.1.3 Precarity as sum score

Lastly, we examine the relationships between individual symptoms and overall precarity, an aggregated measure represented by the sum of five precariousness factors. This analysis provides a complementary perspective, capturing broader patterns that may not be evident in the disaggregated symptom-precariousness analysis. By aggregating precariousness factors into a single score, this approach may capture distributed relationships across different precarity factors that were

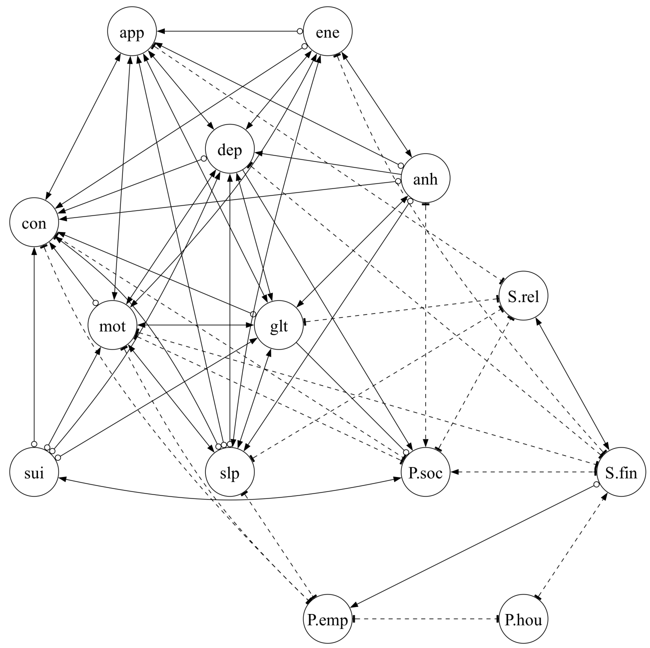

(a) FCI PAG

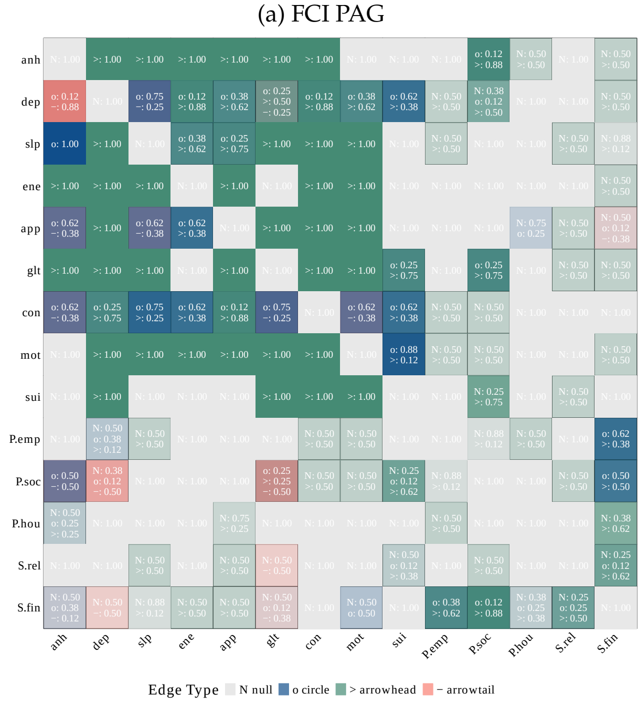

(b) Proportion matrix

Figure 6: Resulting graph of precarity factors and individual depression symptoms using FCI and proportion of edge endpoint types.

previously overlooked in the disaggregated analysis.

Unlike the disaggregated graph in Figure 6, the aggregated symptom-precariousness graph (Figure 7 panel (a)) shows more certainty in causal directions, with only a few edges resulting in ties, all of which involve the overall precarity factor. This is even more evident in the proportion matrix (Figure 7 panel (b)), where symptom-to-symptom interactions almost fully converge to a single edge type. Additionally, all symptom interactions are connected either through bidirectional edges or a combination of an arrowhead and a circle, suggesting a strong presence of latent confounders.

Examining the symptom-precarity connections, we observe a stronger overall trend of depressive symptoms influencing precarity, rather than the other way around. Specifically, anh, dep, and slp show a high probability of causing precarity, whereas app, glt, and mot exhibit more uncertainty in directionality, often resulting in circle endpoints. This pattern suggests that when precariousness factors are aggregated, the dominant causal flow is from depressive symptoms to precarity, rather than precarity driving depression. Particularly, dep emerges as the strongest predictor of precarity, exhibiting the highest proportion of arrowtails, consistent with findings from the disaggregated analysis.

Comparing this with the CCI-derived graph (Figure 12), several key differences stand out. The CCI results reveal that most symptoms are interconnected through bidirectional edges, suggesting a strong presence of latent confounders. However, dep appears to be a distinct exception, as it is predominantly caused by nearly all other symptoms, with one exception sui, which does not contribute to dep. Similarly, con is influenced by multiple symptoms, albeit with weaker support compared to dep. Most interestingly, the CCI results highlight a distinct feedback loop between dep and overall precarity, represented by a tail-tail edge (—). This suggests a possible reinforcing cycle between depression and overall precariousness, where depression not only arises from precarious conditions but also contributes to their persistence, creating a self-sustaining dynamic.

Overall, the aggregated precariousness graph supports the key findings from both the disaggregated analysis and the depression sum score analysis, providing greater certainty in several important patterns. The results highlight the significant role of latent confounders in symptom-to-symptom interactions. While certain stressor-related precariousness factors, particularly S.fin and S.rel, appear to causally influence depressive symptoms, other precariousness factors are more likely driven by depression rather than acting as primary causes, suggesting that precariousness may function more as a consequence of depression than its source. Some symptoms, particularly glt, slp, and dep, show greater sensitivity to precarious conditions, while also playing a central role in symptom dynamics. Among them, slp and glt emerge as influential symptoms within the depression network, whereas con and dep, despite their high connectivity, behave more as outcomes rather than primary drivers. Together, these findings suggest that depression—especially symptoms like sleep disturbances and guilt—may contribute to sustaining precarious conditions, possibly forming a reciprocal cycle between depression and precariousness.

3.2 Simulating the Dynamics Between Precarity and Depression Under Intervention

To evaluate how internal system structure influences the effect of external support, we simulated outcomes under a range of intervention strengths across the top 30 parameter sets from the calibrated model ensemble. The top panel of Figure 8 shows mean levels of depression (D) and precarity (P) after simulation, with each line representing one parameter set. Lines are color-coded by combined feedback and input strength, calculated as the product $\alpha_1 \times \alpha_2 \times \beta_1 \times \beta_2$.

Parameter sets with stronger interactions exhibit more pronounced declines in both depression and precarity in response to intervention. At full intervention—modeled as a complete shift of external stress (S) toward its observed minimum—the mean depression level decreases from -0.113 to -0.963, and precarity from -0.100 to -0.958. These changes correspond to reductions of approximately 90.8% relative to their initial magnitudes, indicating that targeted intervention can shift the system toward a substantially lower-risk equilibrium.

To better understand these dynamics, we focused on two illustrative parameter sets: one with strong feedback/input coupling and low noise (a "bistable" candidate), and one with weaker coupling and higher noise (a "unistable" candidate). In nonlinear systems, bistability refers to the existence of two distinct stable equilibria—meaning the system's long-term outcome depends on its starting point or perturbations.

In our model, bistability arises from the interaction between strong internal coupling—particularly the product $\alpha_2 \times \beta_2$—and the system's nonlinearity. The $\tanh(\cdot)$ activation function saturates at high input values, meaning sufficient gain is required to push the system into nonlinear regimes where multiple stable points emerge. If the feedback gain is too low, or the system is overwhelmed by noise, it behaves more linearly and settles into a single equilibrium—yielding a unistable configuration.[1]

The bottom panel of Figure 8 illustrates these contrasting behaviors. In the bistable model, a clear bifurcation emerges: small interventions have little effect, but once a threshold is crossed, the system abruptly transitions to a low-risk state. In the unistable model, the transition is gradual and continuous, with outcomes improving incrementally as stress is reduced.

These findings underscore that the impact of intervention depends not only on its intensity, but on the system's internal configuration. In bistable regimes, small or moderate interventions may be insufficient unless they push the system

[1]This resembles a classic *pitchfork bifurcation* in discrete dynamical systems: when the gain k in a scalar map like $x_{t+1} = \tanh(kx_t)$ exceeds a critical value, the system shifts from a single fixed point to two stable attractors and one unstable one. In our model, high values of $\alpha_2 \times \beta_2$ similarly enable the emergence of multiple attractor states.

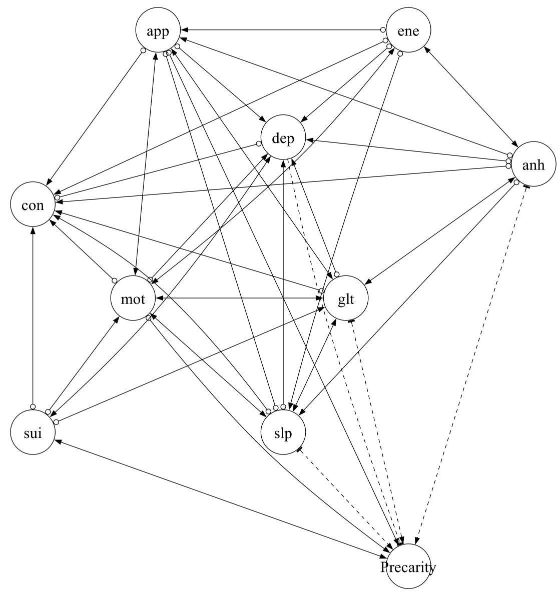

(a) FCI PAG

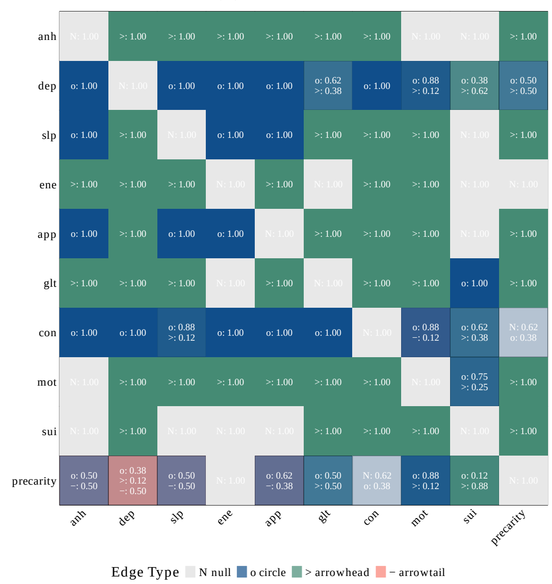

(b) Proportion matrix

Figure 7: Resulting graph of precarity sum score and individual depression symptoms using FCI and proportion of edge endpoint types.

past a tipping point. Unistable systems, by contrast, respond more linearly, offering greater predictability and flexibility in designing incremental interventions.

This distinction is especially relevant for mental health interventions in populations exposed to persistent stressors like housing instability, financial strain, or job insecurity. In such contexts, external adversity may be reinforced through internal feedback loops between psychological distress and precarious conditions. Recognizing when a system is bistable may help identify when strong, early, or multifaceted interventions are needed to produce lasting change—while unistable dynamics may justify more gradual or targeted efforts.

Tailoring intervention strategies to the system's underlying structure may enhance their effectiveness and sustainability, particularly in addressing the compounding effects of socioeconomic precarity on mental health.

4 Discussion

This study combined constraint-based causal discovery and dynamical modeling to investigate how depression and socioeconomic precarity interact—and how their internal structure modulates responsiveness to intervention. Using cross-sectional data from the HELIUS study, we applied cycle-capable discovery algorithms to estimate plausible directional relationships among financial stress, multiple domains of precariousness, and depressive symptoms. By analyzing both aggregate constructs and individual variables, we aimed to capture patterns that may be masked in either extreme of abstraction (i.e., purely aggregate or disaggregated analyses).

The causal analysis consistently identified financial stress (*S.fin*) as a key plausible driver of depression, appearing across both aggregated and disaggregated models. At the symptom level, we found that sleep disturbance (*slp*), depressed mood (*dep*), guilt (*glt*), and anhedonia (*anh*) were especially sensitive to external stressors. Among these, *dep* emerged as a central hub: not only was it heavily influenced by other symptoms, it also exerted directional influence on social precarity (*P.soc*), suggesting a feedback loop in which worsening mood contributes to social disconnection, which in turn may exacerbate depressive symptoms. The CCI algorithm even suggested a possible cyclic relationship between dep and overall precarity, hinting at a structurally self-reinforcing mechanism. *Slp* also played a key initiating role. It showed directed connections to both social and employment precarity and exhibited many outgoing edges within the symptom network. This suggests *slp* may function as an early warning signal or entry point into the depression–precarity cycle, making it a promising target for preventive intervention. In contrast, *P.soc* more often appeared as an effect rather than a cause—receiving arrows from symptoms like *dep* and *glt*, but rarely sending them. This asymmetry implies that social precarity may often reflect downstream consequences of worsening mental health rather than being its root cause. These patterns offer actionable insights for intervention. Addressing

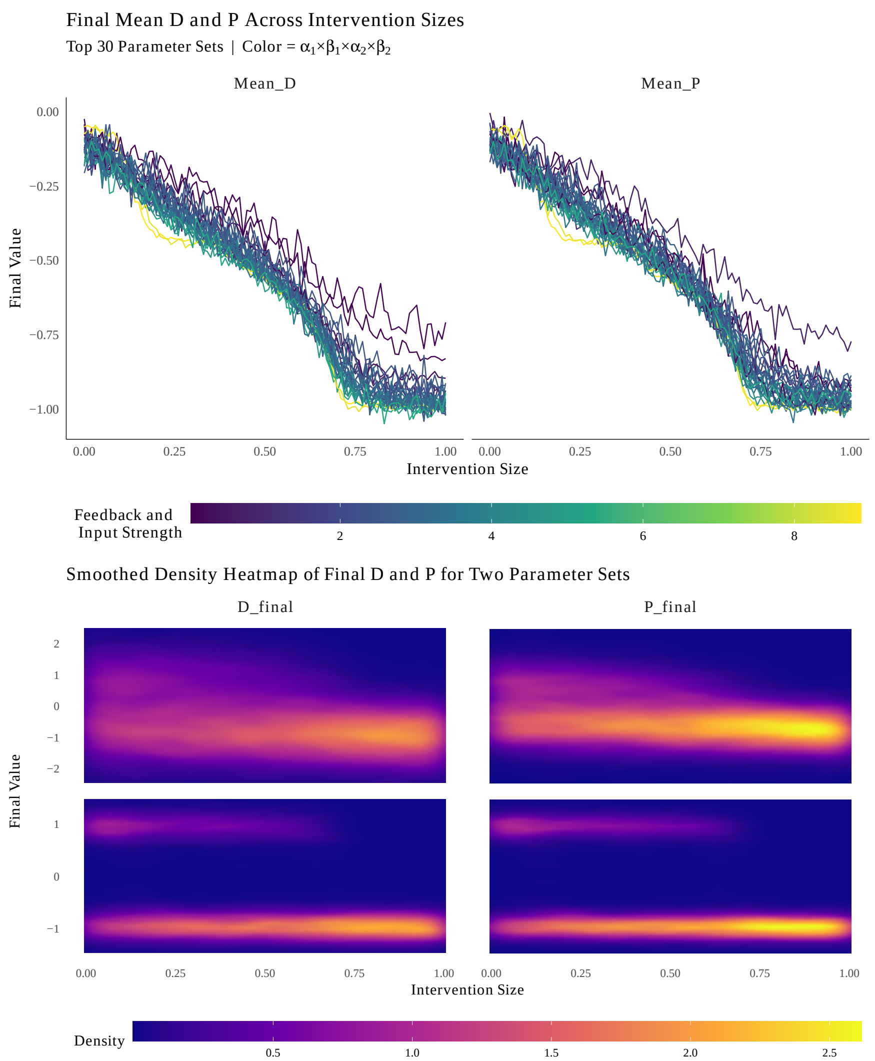

Figure 8: **Top**: Final Mean D and P Across Intervention Sizes. *Mean trajectories of depression (D) and precarity (P) across varying intervention strengths, simulated over the top 30 parameter sets. Each line represents one parameter set and is colored by its combined feedback and input strength.* **Bottom**: Smoothed Density Heatmap of Final D and P for Two Parameter Sets. *One exhibits unistability (top two panels) and the other exhibits bistability (bottom two panels). Bistable dynamics reveal a sharp transition between distinct outcome regimes, while unistable dynamics show gradual, continuous change across the intervention gradient.*

symptoms like *slp* early may prevent escalation into broader depressive states or worsening precarity. Intervening on *dep*, as a central node with potential feedback effects, could also disrupt the self-reinforcing dynamics between mental health and social isolation.

To examine how such structures shape responsiveness to support, we developed a simplified two-variable nonlinear dynamical model capturing the feedback between depression and precarity, modulated by financial stress. Calibrated against empirical summary statistics from the HELIUS dataset, the model allowed us to simulate how these dynamics evolve under varying levels of stress reduction. The simulations revealed that intervention effectiveness depends not just on the magnitude of external stressors, but on the internal configuration of the system itself. In bistable regimes—characterized by strong feedback and low noise—the system could remain stuck in a high-risk state unless an intervention crosses a critical threshold, tipping it into a healthier equilibrium. By contrast, unistable systems—driven by weaker coupling or greater noise—responded more gradually and proportionally to increasing support. These dynamics carry practical policy implications. In bistable systems, even moderate interventions may have little effect unless they are forceful enough to tip the system toward a lower-risk state. This underscores the importance of early or intensive support when targeting self-reinforcing cycles of depression and precarity. Unistable systems, by contrast, are more responsive to incremental support, suggesting that sustained, moderate interventions may be sufficient in such contexts.

That said, our study has several limitations. While the FCI and CCI algorithms are designed to recover causal structure from cross-sectional data—including feedback and latent confounding—many edge directions in our results remain ambiguous, as indicated by the prevalence of circle endpoints and bidirectional arrows, especially in weakly connected regions of the graph. These uncertainties were most evident in the links between individual symptoms and precariousness factors, where edge estimates varied across algorithms and conditional independence (CI) tests. This likely reflects limited statistical signal in high-dimensional settings, where large conditioning sets reduce power and small effect sizes are harder to detect. Although the CCI algorithm is explicitly designed to detect cycles, we found little clear evidence of feedback: most candidate loops appeared only as bidirectional edges, which may reflect latent confounding or statistical imprecision rather than true cyclic structure. This could point to either an absence of strong feedback at the symptom level or limitations in the sensitivity of full-graph discovery approaches applied to densely interconnected variables. More focused strategies, such as local structure tests or theory-guided subgraph modeling, may help resolve these ambiguities. In addition, while our analyses relied solely on observational data, some structural uncertainties—particularly those involving latent confounding or bidirectional influence—may ultimately require interventional or semi-interventional designs. Extensions such as LLC (Hyttinen et al., 2012), NODAGS-Flow (Sethuraman et al., 2023), or Bicycle (Rohbeck et al., 2024), which integrate observational and interventional data, may prove valuable where such data are available.

Second, our findings showed sensitivity to the choice of conditional independence (CI) test. The Gaussian CI test, which assumes linear relationships and Gaussian noise, often produced denser graphs—likely due to its tendency to overestimate weak or noisy linear associations. In contrast, RCoT, a nonparametric alternative, avoids these assumptions but relies on a Gaussian radial basis function (RBF) kernel to assess dependence. While flexible in capturing nonlinear relationships, this kernel is optimized for smooth, continuous variables and may underperform with discrete or ordinal data. Its similarity estimates can be unreliable when applied to variables with discontinuities, potentially leading to missed dependencies—particularly relevant in the HELIUS dataset, where some variables are ordinal or mixed-type (Howlett, 2001). To address this, future work should consider adapting kernel-based CI tests to better handle mixed data structures—for example, by employing hybrid kernels that explicitly combine continuous and discrete similarity measures. This could improve the reliability of nonparametric causal discovery in settings with heterogeneous variable types.

Finally, the structure of the dynamical model introduces its own limitations. While the model was designed to reflect key features of the discovered causal structure, it represents a highly simplified system: only two variables—depression and social precarity—modulated by external financial stress. This abstraction allowed for tractable analysis and visual intuition, particularly around nonlinear behaviors such as bistability, but omits other potentially influential constructs highlighted in the causal graphs, including relational stress, employment conditions and housing conditions. Moreover, the model's nonlinearity—introduced via the hyperbolic tangent function—was chosen for convenience rather than empirical justification. While this function supports saturation and the emergence of tipping points, the presence of bistability is a product of simulation, not empirical verification. It remains possible that simpler, linear dynamics could account for the observed data just as well. Future work should further investigate whether bistability is a necessary feature of depression–precarity dynamics, and explore alternative functional forms—both linear and nonlinear—using richer data and stronger empirical constraints.

Our results reveal that the effectiveness of interventions targeting depression and precarity is shaped not only by the strength of external stressors but also by the internal structure of the system. The interplay between feedback strength and noise determines whether a system responds gradually or only after crossing a tipping point—highlighting the need for intervention strategies attuned to these underlying dynamics.

These findings underscore the importance of considering internal feedback—not just external adversity—when designing interventions. Mental health systems are not always passively responsive to support; their structure can constrain how much impact any given policy has. By diagnosing these structural features—through tools like causal discovery and computational modeling—researchers and policymakers can better tailor interventions to the underlying mechanics of vulnerability.

Beyond these specific findings, this study offers a generalizable framework for studying complex mental health phenomena. Causal discovery enables principled hypothesis generation from observational data, while dynamical modeling helps test how those structures behave under intervention. Together, these methods move us from descriptive patterns to mechanistic insight, with practical relevance for real-world mental health policy.

Future work could build richer dynamical models grounded in higher-resolution empirical data—potentially incorporating time, interventions, or more granular psychosocial constructs. Such extensions would help validate whether mechanisms proposed here, such as bistability, manifest in real-world trajectories. Ultimately, we hope this study encourages further integration of causal structure learning and system-level modeling to improve mental health outcomes under conditions of socioeconomic precarity.

5 References

Deb, K., Pratap, A., Agarwal, S., & Meyarivan, T. (2002). A fast and elitist multiobjective genetic algorithm: NSGA-II. *IEEE Transactions on Evolutionary Computation*, *6*(2), 182–197.

Dojer, N. (2016). Learning bayesian networks from datasets joining continuous and discrete variables. *International Journal of Approximate Reasoning*, *78*, 116–124.

Elsenburg, L. K., Nicolaou, M., Galenkamp, H., Lakerveld, J., & Stronks, K. (2025). The clustering of disadvantage in different life dimensions across ethnic groups: A network analysis of indicators of precariousness in the HELIUS study. *Social Science & Medicine*, 117970.

Entner, D., & Hoyer, P. O. (2010). On causal discovery from time series data using FCI. *Probabilistic Graphical Models*, *16*.

Fone, D., White, J., Farewell, D., Kelly, M., John, G., Lloyd, K., Williams, G., & Dunstan, F. (2014). Effect of neighbourhood deprivation and social cohesion on mental health inequality: A multilevel population-based longitudinal study. *Psychological Medicine*, *44*(11), 2449–2460.

Forré, P., & Mooij, J. M. (2018). Constraint-based causal discovery for non-linear structural causal models with cycles and latent confounders. *arXiv Preprint arXiv:1807.03024*.

Franz, R., & Nakamura, R. (2015). *nsga2R: Elitist non-dominated sorting genetic algorithm for multi-objective optimization*. https://CRAN.R-project.org/package=nsga2R

Galenkamp, H., Stronks, K., Snijder, M. B., & Derks, E. M. (2017). Measurement invariance testing of the PHQ-9 in a multi-ethnic population in europe: The HELIUS study. *BMC Psychiatry*, *17*, 1–14.

Gruebner, O., Rapp, M. A., Adli, M., Kluge, U., Galea, S., & Heinz, A. (2017).

Cities and mental health. *Deutsches Ärzteblatt International*, *114*(8), 121.
Howlett, R. J. (2001). *Radial basis function networks 1: Recent developments in theory and applications*.
Hyttinen, A., Eberhardt, F., & Hoyer, P. O. (2012). Learning linear cyclic causal models with latent variables. *The Journal of Machine Learning Research*, *13*(1), 3387–3439.
Lindsay, B. G., Pilla, R. S., & Basak, P. (2000). Moment-based approximations of distributions using mixtures: Theory and applications. *Annals of the Institute of Statistical Mathematics*, *52*, 215–230.
Mooij, J. M., & Claassen, T. (2020). Constraint-based causal discovery using partial ancestral graphs in the presence of cycles. *Conference on Uncertainty in Artificial Intelligence*, 1159–1168.
Neapolitan, R. E. et al. (2004). *Learning bayesian networks* (Vol. 38). Pearson Prentice Hall Upper Saddle River.
Park, K., Waldorp, L. J., & Ryan, O. (2024). Discovering cyclic causal models in psychological research. *Advances. In/Psychology*, *2*, e72425.
Park, K., Waldorp, L., & Vasconcelos, V. V. (2025). *The individual-and population-level mechanistic implications of statistical networks of symptoms*.
Pevalin, D. J., Reeves, A., Baker, E., & Bentley, R. (2017). The impact of persistent poor housing conditions on mental health: A longitudinal population-based study. *Preventive Medicine*, *105*, 304–310.
Rahimi, A., & Recht, B. (2007). Random features for large-scale kernel machines. *Advances in Neural Information Processing Systems*, *20*.
Rehm, J., & Shield, K. D. (2019). Global burden of disease and the impact of mental and addictive disorders. *Current Psychiatry Reports*, *21*, 1–7.
Rohbeck, M., Clarke, B., Mikulik, K., Pettet, A., Stegle, O., & Ueltzhöffer, K. (2024). Bicycle: Intervention-based causal discovery with cycles. In F. Locatello & V. Didelez (Eds.), *Proceedings of the third conference on causal learning and reasoning* (Vol. 236, pp. 209–242). PMLR.
Rönnblad, T., Grönholm, E., Jonsson, J., Koranyi, I., Orellana, C., Kreshpaj, B., Chen, L., Stockfelt, L., & Bodin, T. (2019). Precarious employment and mental health. *Scandinavian Journal of Work, Environment & Health*, *45*(5), 429–443.
Rugulies, R., Aust, B., Greiner, B. A., Arensman, E., Kawakami, N., LaMontagne, A. D., & Madsen, I. E. (2023). Work-related causes of mental health conditions and interventions for their improvement in workplaces. *The Lancet*, *402*(10410), 1368–1381.
Runge, J., Nowack, P., Kretschmer, M., Flaxman, S., & Sejdinovic, D. (2019). Detecting and quantifying causal associations in large nonlinear time series datasets. *Science Advances*, *5*(11), eaau4996.
Sethuraman, M. G., Lopez, R., Mohan, R., Fekri, F., Biancalani, T., & Hütter, J.-C. (2023). NODAGS-flow: Nonlinear cyclic causal structure learning. *International Conference on Artificial Intelligence and Statistics*, 6371–6387.
Snijder, M. B., Galenkamp, H., Prins, M., Derks, E. M., Peters, R. J., Zwinderman, A. H., & Stronks, K. (2017). Cohort profile: The healthy life in an urban setting (HELIUS) study in amsterdam, the netherlands. *BMJ Open*, *7*(12),

e017873.
Spirtes, P., Glymour, C., & Scheines, R. (2001). *Causation, prediction, and search*. MIT press.
Spirtes, P., Meek, C., & Richardson, T. (1995). Causal inference in the presence of latent variables and selection bias. *Proceedings of the Eleventh Conference on Uncertainty in Artificial Intelligence*, 499–506.
Storn, R., & Price, K. (1997). Differential evolution–a simple and efficient heuristic for global optimization over continuous spaces. *Journal of Global Optimization*, *11*, 341–359.
Strobl, E. V. (2019). A constraint-based algorithm for causal discovery with cycles, latent variables and selection bias. *International Journal of Data Science and Analytics*, *8*(1), 33–56. https://doi.org/10.1007/s41060-018-0158-2
Strobl, E. V., Zhang, K., & Visweswaran, S. (2019). Approximate kernel-based conditional independence tests for fast non-parametric causal discovery. *Journal of Causal Inference*, *7*(1), 20180017.
Stronks, K., Snijder, M. B., Peters, R. J., Prins, M., Schene, A. H., & Zwinderman, A. H. (2013). Unravelling the impact of ethnicity on health in europe: The HELIUS study. *BMC Public Health*, *13*, 1–10.
Van Der Wal, J. M., Van Borkulo, C. D., Deserno, M. K., Breedvelt, J. J., Lees, M., Lokman, J. C., Borsboom, D., Denys, D., Holst, R. J. van, Smidt, M. P., et al. (2021). Advancing urban mental health research: From complexity science to actionable targets for intervention. *The Lancet Psychiatry*, *8*(11), 991–1000.
World Health Organization. (2022). *Mental disorders*. World Health Organization. https://www.who.int/news-room/fact-sheets/detail/mental-disorders
Zhang, K., Peters, J., Janzing, D., & Schölkopf, B. (2012). Kernel-based conditional independence test and application in causal discovery. *arXiv Preprint arXiv:1202.3775*.

6 Appendix

6.1 HELIUS study

The HELIUS (HEalthy LIfe in an Urban Setting) study is a large-scale, multiethnic cohort study conducted in Amsterdam. Participants were randomly selected from the municipality register and stratified by ethnic origin to ensure balanced representation across six major groups. Invitation letters were sent by mail, followed by a reminder after two weeks. Non-respondents were contacted via home visits where applicable.

Of those invited, approximately 55% responded (Dutch: 55%, Surinamese: 62%, Ghanaian: 57%, Turkish: 46%, Moroccan: 48%). Among those contacted, 50% agreed to participate (Dutch: 60%, Surinamese: 51%, Ghanaian: 61%, Turkish: 41%, Moroccan: 43%), resulting in an overall participation rate of 28%.

Participants completed either a digital or paper version of the questionnaire, with assistance offered when needed, and received a confirmation letter for a physical examination appointment.

At baseline (2011–2015), 24,780 individuals were enrolled. Of these, 23,936 participants completed the questionnaire that included items relevant to precariousness. After excluding individuals with missing data on key variables, the final analytical sample consisted of 21,628 participants.

The HELIUS study received approval from the Medical Ethics Committee of the Academic Medical Center (AMC), and written informed consent was obtained from all participants prior to enrollment.

6.2 Causal Discovery Primer

As shown in Table 1, the resulting graphs from FCI and CCI differ slightly (*PAG*: partial ancestral graph; *MAAG*: maximal almost ancestral graph) due to their reliance on different underlying assumptions. Despite these differences, both graphs belong to the class of *ancestral graphs*, which are designed to encode causal relationships between variables, where the presence of an edge indicates causal *ancestry.* In these graphs, directed edges, $A{*}\!\!\rightarrow\!B$, indicate that B is not an ancestor of A in every graph within the Markov equivalence class, $Equiv(G)$. The Markov equivalence class represents a set of graphs that encode the same conditional independence relationships, ensuring that the same *d-separation* conditions hold across all graphs in the class (Spirtes et al., 2001). Conversely, an edge marked as $A{*}\!\!-\!B$ indicates that B is an ancestor of A across all graphs in $Equiv(G)$. Circle endpoints, $A{*}\!\!-\!\!\circ B$, represent ambiguity in the ancestral relationship, meaning B's ancestral status relative to A varies across graphs in $Equiv(G)$.[2] Finally, when an edge is represented as $A\leftrightarrow B$, it implies that neither A nor B is an ancestor of the other, suggesting the presence of a latent confounder influencing both variables.

Table 1: Assumptions of causal discovery algorithms

Algorithm	Acyclicity	Causal sufficiency	Absence of selection bias	Linearity	Output
PC	✓	✓	✓	✓	CPDAG
FCI	–[a]	✓	–[a]	–[a]	PAG
CCI	x	x	x	✓	(partially oriented) MAAG

Note. [a]The FCI algorithm, introduced by Spirtes (1995), is a constraint-based causal discovery method for DAGs that accounts for latent confounding and selection bias. Mooij & Claassen (2020) later showed its applicability to cyclic causal discovery with latent confounding under general faithfulness and Markov conditions, assuming non-linear causal relationships.

The algorithms also differ in how they detect cycles and represent cyclic rela-

[2]$*$ serves as a *meta-symbol*, representing one of the three possible edge-endpoints. For instance, $A\!-\!\!*B$ can indicate any of the following edges: $A - B$, $A\longrightarrow B$, or $A\!-\!\!\circ B$ (Park et al., 2024).

tionships in their resulting graphs. In CCI's MAAG, A — B indicates that A is an ancestor of B, and simultaneously B is an ancestor of A, referring to a cyclic relationship between $A \leftrightarrows B$. FCI, on the other hand, identifies potential cycles more subtly. In its PAG, fully-connected nodes with circle endpoints ($\circ\!-\!\circ$) may suggest the presence of cyclic structures. FCI, therefore, provides a sufficient condition to distinguish variables that are not part of a cycle, offering a more nuanced approach to handling cyclic relationships (Mooij & Claassen, 2020).

Table 1 highlights further differences in the assumptions underlying these algorithms. CCI operates under the assumption of a linear system, whereas FCI, particularly when used to infer cyclic relationships, assumes a non-linear system without selection bias and adheres to more general faithfulness and Markov conditions (i.e., *σ-separation* and *σ-faithfulness* setting) (Forré & Mooij, 2018). When the respective assumptions of each algorithm are met, their inferred cyclic relationships align with those illustrated in Figure 9.

While CCI's MAAG provides an explicit representation of cyclic relationships, it has certain theoretical limitations, as the MAAG may not always fully preserve d-separation relations from the original graph, $\mathcal{G}$ (Strobl, 2019). Given these considerations, we examine and compare results from both algorithms, placing more weight on the FCI results, which are presented in the main results section, while discussing CCI results where relevant, with detailed findings provided in the Appendix. A full discussion of causal discovery concepts and algorithmic details is beyond the scope of this paper; however, readers seeking a more in-depth understanding can refer to Park et al. (2024) for a comprehensive exploration of these methods and their applications.

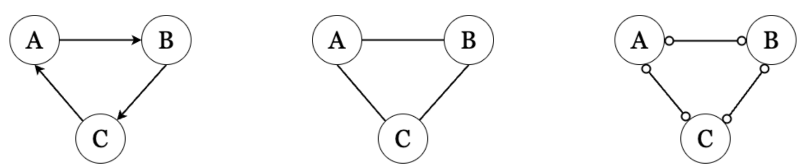

(a) Example graph $\mathcal{G}$ (b) Corresponding MAAG (c) Corrsponding PAG

Figure 9: Example graph $\mathcal{G}$ featuring a cycle and the corresponding MAAG from CCI and PAG from FCI.

The graph produced by the PC algorithm is a *CPDAG* (completed partially directed acyclic graph), where directed edges ($A \to B$) indicate that A is a direct cause (parent) of B. Unlike FCI and CCI, the CPDAG does not include circle symbols. Instead, when the PC algorithm cannot determine the direction of causality, it represents this uncertainty with bidirectional arrows. While the PC algorithm serves as a useful reference, its strict assumptions — acyclicity and the absence of latent confounders—limit its applicability in more complex scenarios. For this reason, our primary focus remains on the results obtained from FCI and CCI, with all PC algorithm results provided in the Appendix for completeness.

6.3 Precariousness factors by Leonie

1. EMPLOYMENT PRECARIOUSNESS

- `H1_Arbeidsparticipatie`: Working status
- `H1_WerkSit`: Which work situation most applies to you?
- `H1_RecentErv8`: Experiences past 12 months: h. You were sacked from your job or became unemployed (*reverse*)

2. FINANCIAL PRECARIOUSNESS

- `H1_InkHhMoeite`: During the past year, did you have problems managing your household income?
- `H1_RecentErv9`: Experiences past 12 months: i. You had a major financial crisis (*reverse*)

3. HOUSING PRECARIOUSNESS

- `veilig_2012`: Score safety (veiligheid) in 2012 (*reverse*)
- `vrz_2012`: Score level of resources (niveau voorzieningen) in 2012 (*reverse*)
- `P_HUURWON`: Percentage Huurwoningen

4. CULTURAL PRECARIOUSNESS

- `H1_Discr_sumscore`: Perceived discrimination: sum score of 9 items (range 9-45)
- `H1_SBSQ_meanscore`: Health literacy: SBSQ meanscore (range 1-5) (*reverse*)
- `A_BED_RU`: Aantal bedrijfsvestigingen; cultuur, recreatie, overige diensten (*reverse*)

5. SOCIAL PRECARIOUSNESS

- `H1_RecentErv5`: Experiences past 12 months: e. Your steady relationship ended (*reverse*)
- `H1_RecentErv6`: Experiences past 12 months: f. A long-term friendship with a good friend or family member was broken off (*reverse*)
- `H1_RecentErv7`: Experiences past 12 months: g. You had a serious problem with a good friend or family member, or neighbour (*reverse*)
- `H1_SSQT`: SSQT (frequency of social contact): sum score of 5 items (range 5-20) (*reverse*)
- `H1_SSQSa`: SSQS (adequacy of social contact): sum score of 5 items, category 3 and 4 not combined (range 5-20) (*reverse*)

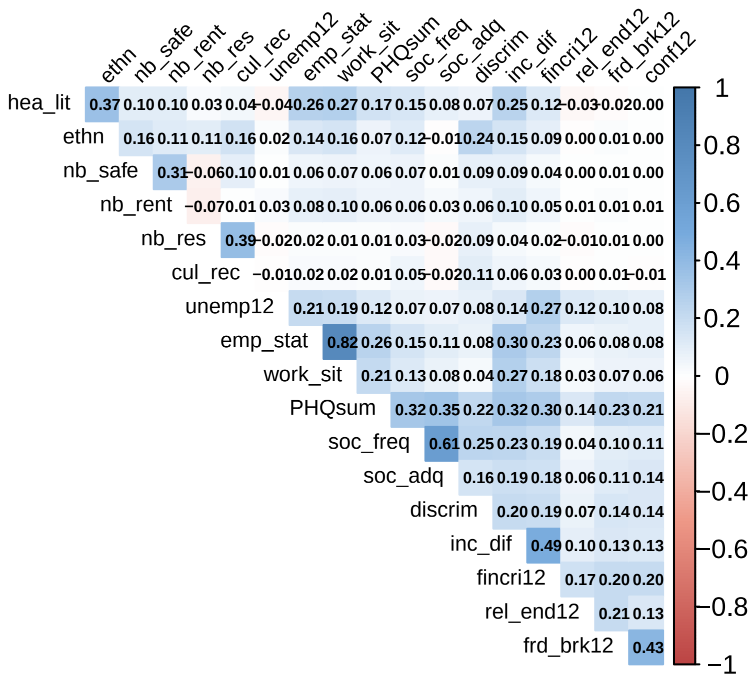

- **High** Correlations: `emp_stat` (employment status) and `work_sit` (work situation) have a strong positive correlation of 0.82. This suggests that individuals with higher employment status tend to have more secure or favorable work situations. `soc_freq` (social contact frequency) shows a strong positive correlation with `soc_adq` (social adequacy) at 0.61. This indicates that individuals with more frequent social contact also tend to have higher perceived adequacy of social interactions.

- **Moderate** Correlations: `nb_safe` (neighborhood safety) and `nb_res` (resources) have a moderate positive correlation of 0.39, suggesting that areas with higher safety also have better resources. `hea_lit` (health literacy) has moderate correlations with `emp_stat` (0.26) and `work_sit` (0.25), which could mean that higher health literacy is associated with better employment situations. `frd_brk12` (friendship breakups) and `conf12` (conflicts) have a notable correlation of 0.43, indicating a relationship between having conflicts and friendship losses.

- **Low to Moderate** Correlations in Financial Precariousness: `inc_dif` (income difficulties) has a moderate correlation with `fincri12` (financial crisis) at 0.49. This aligns with the expected relationship, where individuals who experience general income difficulties are more likely to report financial crises.

- **Low** Correlations (0.1 - 0.2): Many variables, such as `discrim` (discrimination), `unemp12` (unemployment experience), and `rel_end12` (relationship end), have low correlations with other variables, suggesting relatively independent relationships in the context of this dataset.

6.4 Exploratory Factor Analysis (EFA)

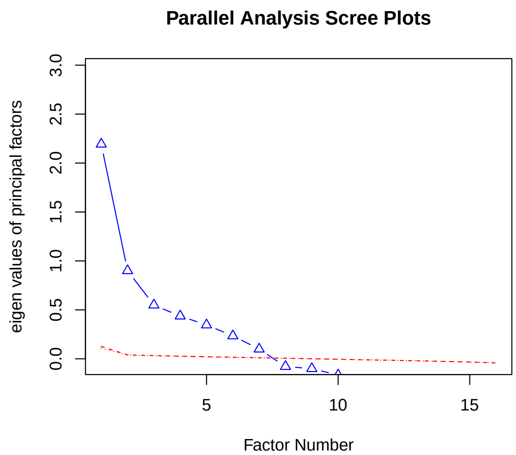

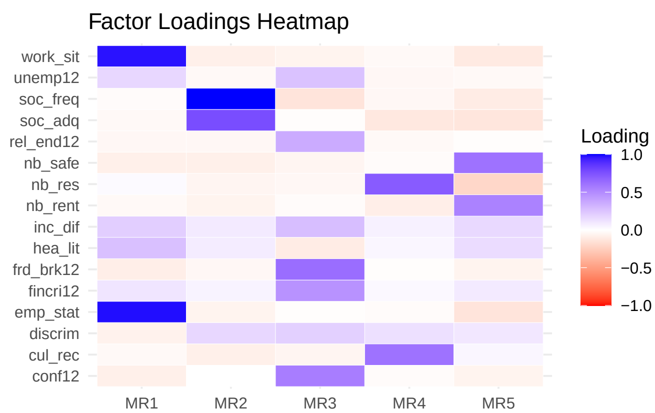

6.4.1 Factor Loadings (Pattern Matrix)

- **MR1**: High loadings on `emp_stat` and `work_sit` suggest this factor captures *employment* precariousness.
- **MR2**: Strong loadings on `soc_freq` and `soc_adq` indicate *social* precariousness.
- **MR3**: Key items like `frd_brk12`, `conf12`, and `fincri12`, suggest recent *stressful events*.
- **MR4**: High loadings on `nb_res` and `cul_rec` may reflect *community resources* precariousness.
- **MR5**: Variables `nb_safe` and `nb_rent` with high loadings indicate *housing* precariousness.

6.4.2 Variance Explained

The factors cumulatively explain **38%** of the variance, with MR1 being the most influential factor. Each factor contributes a smaller proportion to the total variance (MR1 at 12%, MR2 at 9%, etc.).

6.4.3 Factor Intercorrelations

Factors are moderately correlated, especially between *MR1 and MR5*, and *MR2 and MR3*. This indicates that while distinct, these factors are related—reasonable in a complex socio-economic context.

6.4.4 Model Fit Statistics

RMSEA (0.071) suggest an acceptable fit. Tucker Lewis Index (0.802) suggests moderate reliability for the model.

6.4.5 Summary

The 5-factor model appears interpretable and captures distinct dimensions of precariousness: *employment, social, stressors, community resources, and housing precariousness*. Although the overall fit and explained variance could be stronger, these factors offer insights into the underlying structure of the data, highlighting key areas of precariousness.

6.5 PCA

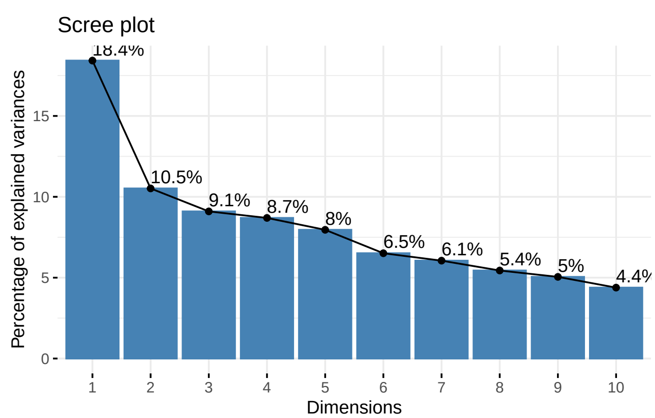

- Component Retention: The scree plot shows a clear "elbow" after the first component. This steep drop suggests that most variance is explained by the first component. After Dimension 5, the percentage of explained variance decreases slightly more gradually, indicating diminishing returns for adding more components. If we need to choose multiple components, retaining the first 5 components seems reasonable, as they capture most of the variance (cumulatively explaining about 54.7% of the total variance).

Contribution of Variables to 5 Principal Components

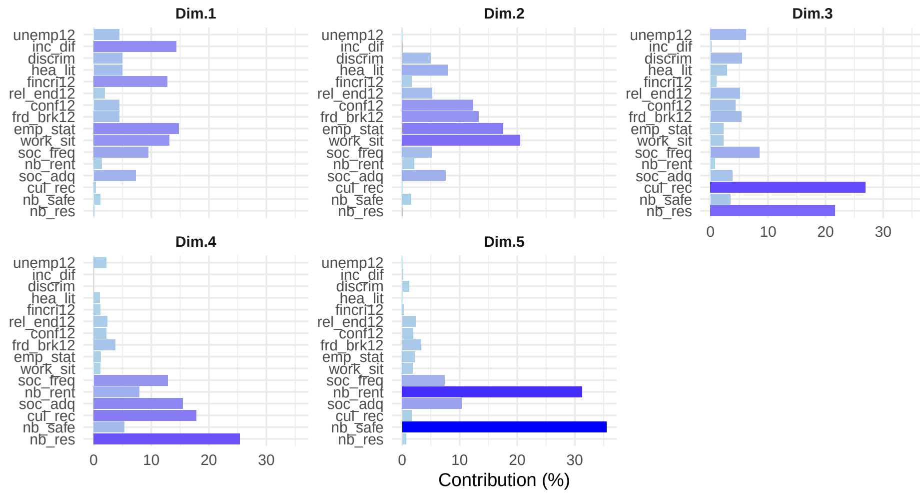

6.5.1 Explained variance (contributions) of variables

It shows the importance of variables within each component.

- **Dim1**: High contributions are observed from `emp_stat`, `work_sit`, `inc_dif`, and `fincri12`, suggesting that this dimension captures aspects of *employment and financial* security.
- **Dim2**: While `emp_stat` and `work_sit` overlap with Dim1, the strong contributions from `frd_brk12` and `rel_end12` indicate that this dimension captures a focus on *recent relationship stressors*.
- **Dim3**: `cul_rec`, `nb_res` have the highest contributions, indicating this dimension likely represents *community and cultural* factors.
- **Dim4**: `soc_freq` and `soc_adq` stand out in this dimension, suggesting an emphasis on *social* precariousness.
- **Dim5**: `nb_safe` and `nb_rent` are the top contributors, pointing to *housing* security as key themes in this component.

6.5.2 Cos² Values

Cos² (squared cosine) values, or the quality of representation, show how well each variable is represented by each dimension. where higher cos² values (closer to 1) indicate better representation of a variable by a component.

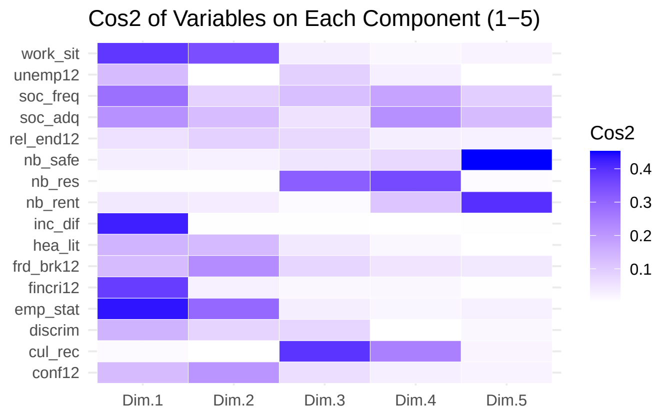

- **Dim.1**: Variables `emp_stat`, `work_sit`, `inc_dif`, and `fincri12` show high cos² values, meaning that PC1 primarily captures variations in employment and financial difficulties. This component could represent *employment & finance* precariousness.
- **Dim.2**: Variables `work_sit`, `emp_stat`, `frd_brk12`, and `conf12` are well-represented in this component, suggesting PC2 captures aspects of *recent relationship stressors*.
- **Dim.3**: Variables `nb_res` and `cul_rec` load strongly on PC3. This may represent community or cultural resources, indicating that this component is associated with *neighborhood resources*.
- **Dim.4**: This component has high cos² values for `nb_res`, `cul_rec`, `soc_freq`, and `soc_adq`. While `nb_res` and `cul_rec` are also prominent in PC3, PC4 uniquely captures nuanced differentiation in *social* precariousness.
- **Dim.5**: `nb_safe` and `nb_rent` are well-represented by PC5. This component might capture *housing* precariousness.

6.6 ICA

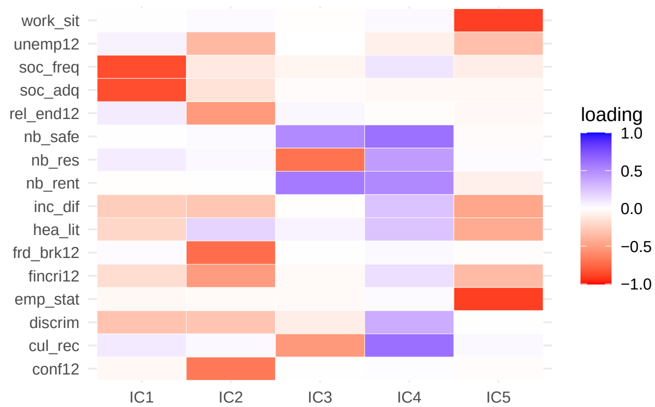

6.6.1 Dominant Variables per Component:

For each Independent Component (IC), we can identify variables with *high absolute* values in each column. These values indicate that the IC captures a strong, independent signal associated with these variables.

- **IC1**: `soc_freq` and `soc_adq` have strong negative loadings on this component, indicating that this component might represent *social* precariousness.
- **IC2**: `frd_brk12`, `conf12`, `rel_end12`, `fincri12` and `unemp12` have the most substantial loadings on this component, all with negative signs. This might point to a *recent relational or social stressor* component.
- **IC3**: `nb_res` and `cul_rec` show notable negative loadings, pointing to a focus on *community resource* precariousness.
- **IC4**: High loadings for `nb_safe`, `nb_rent`, `nb_res`, `cul_rec`, and `discrim` suggest a theme of *housing and community-based* precariousness, reflecting both safety and social challenges within the neighborhood context.
- **IC5**: `emp_stat` and `work_sit` both have strong negative loadings on this component, suggesting it captures *employment* precariousness.

6.7 Hierarchical clustering

6.7.1 Using Euclidean distance

- Ward.D's method: Minimizes the variance within clusters, producing more compact and spherical clusters.
- Single linkage: Groups clusters based on the minimum distance between points.

- Complete linkage: Groups clusters based on the maximum distance between points.
- Average linkage: Uses the average distance between all pairs of points in the two clusters.

6.7.1.1 Consistent Groupings (Across All or Most Methods)

- `emp_stat` and `work_sit`: This pair consistently clusters together across all linkage methods, suggesting that they are closely related variables, likely capturing a similar aspect of the data (possibly employment status or employment-related information).

- `nb_safe`, `nb_res`, and `nb_rent`: These variables are often grouped closely in several methods (especially Ward.D, average, and complete linkage). This suggests a similarity or common theme among them, potentially related to neighborhood or housing precariousness.

- `soc_freq` and `soc_adq`: These two variables frequently cluster together, indicating they likely measure aspects of social frequency and adequacy in similar ways. They appear together in Ward.D, average, and complete linkage.

- `frd_brk12` and `conf12`: These variables are often clustered closely (though they sometimes join with other variables like rel_end12), suggesting they may capture aspects of relationship or social conflict. This pair appears in close proximity, especially in average and Ward.D.

6.7.1.2 Inconsistent Groupings (Variability Across Methods)

- `hea_lit`: This variable shows inconsistent clustering across methods. In Ward.D, it joins with `fincri12`, while in other methods, it's often more isolated or grouped with variables that do not appear similar. This may suggest that `hea_lit` does not strongly correlate with other variables, or it has multidimensional aspects affecting its grouping across methods.

- `discrim`: This variable also shows variable groupings. In Ward.D, it is grouped with `hea_lit`, while in other methods (e.g., complete and single linkage), it clusters differently, sometimes on its own. This variability may indicate that `discrim` has weaker associations with the main clusters in the data or overlaps partially with multiple clusters.

- Social and Financial Variables (`inc_dif`, `fincri12`, `unemp12`): These variables appear together in some methods (e.g., Ward.D clusters `fincri12` and `inc_dif`), but in others, they are spread out. This inconsistency suggests that social and financial variables may not have strong or consistent ties across different methods, perhaps due to capturing different aspects of precariousness.

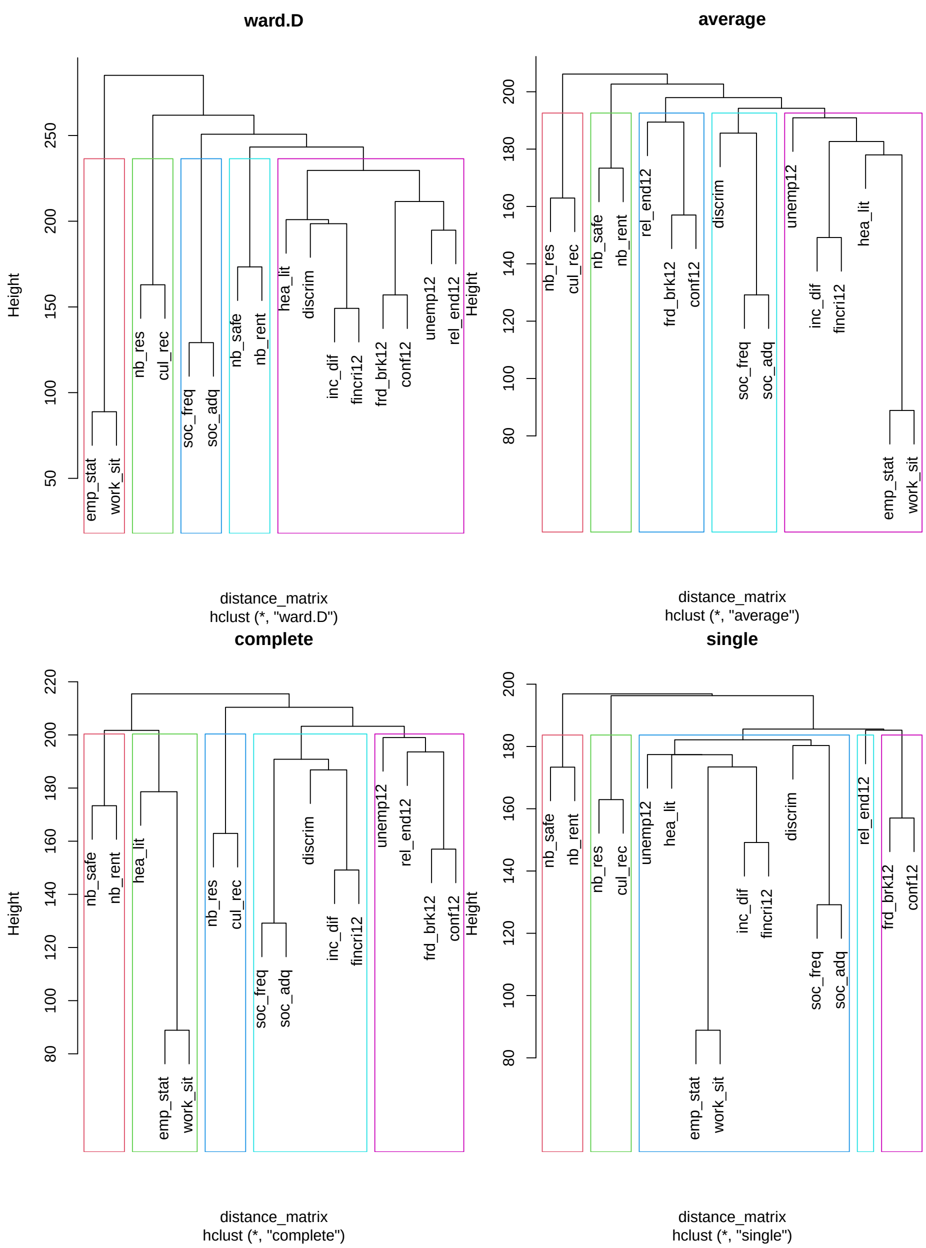
ward.D
Height
emp_stat
work_sit
nb_res
cul_rec
soc_freq
soc_adq
nb_safe
nb_rent
hea_lit
discrim
inc_dif
fincri12
frd_brk12
conf12
unemp12
rel_end12
distance_matrix
hclust (*, "ward.D")
average
nb_res
cul_rec
nb_safe
nb_rent
rel_end12
frd_brk12
conf12
discrim
soc_freq
soc_adq
unemp12
inc_dif
fincri12
hea_lit
emp_stat
work_sit
distance_matrix
hclust (*, "average")
complete
Height
nb_safe
nb_rent
hea_lit
emp_stat
work_sit
nb_res
cul_rec
soc_freq
soc_adq
discrim
inc_dif
fincri12
unemp12
rel_end12
frd_brk12
conf12
distance_matrix
hclust (*, "complete")
single
nb_safe
nb_rent
nb_res
cul_rec
unemp12
hea_lit
emp_stat
work_sit
inc_dif
fincri12
discrim
soc_freq
soc_adq
rel_end12
frd_brk12
conf12
distance_matrix
hclust (*, "single")

6.7.1.3 Summary

The consistent clusters are likely capturing distinct thematic dimensions of the data (e.g., employment, housing, social contact), while the inconsistent variables may reflect multifaceted or weakly correlated attributes that do not fit neatly into one cluster.

6.7.2 Using Mutual Information

Using mutual information (MI) as a basis for hierarchical clustering differs from using traditional distance measures (like Euclidean distance) in a few key ways.

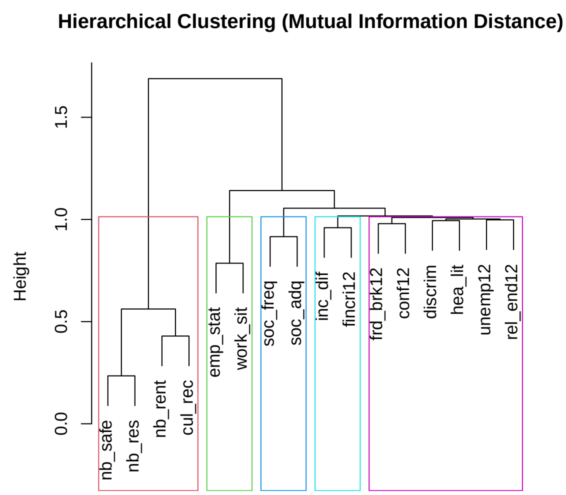

6.7.2.1 Comparison to Euclidean Distance Clustering

- **Housing and Community** Cluster: The variables `nb_safe`, `nb_res`, `nb_rent`, and `cul_rec` cluster together, indicating a strong association among housing-related and community-based factors. This suggests a shared theme of housing or community precariousness. This grouping is also observed in the Euclidean-based clustering, but it appears more tightly connected here, potentially due to the non-linear relationships highlighted by mutual information.
- **Employment and Social Support** Cluster: `emp_stat` and `work_sit` form a cluster, linking employment status and work situation together as they did in Euclidean-based clustering. These remain closely associated regardless of the distance metric used. `soc_freq` and `soc_adq`, related to social contact frequency and adequacy, cluster nearby, indicating they have a stronger non-linear relationship with employment variables. This is a subtle difference as Euclidean distance might not capture this association as effectively.

- **Financial Stressor** Cluster: `inc_dif` and `fincri12`, representing income difficulties and recent financial crises, consistently cluster together in both approaches, showing a strong association, likely linear. However, mutual information-based clustering links these financial stressors with social support variables, suggesting that financial challenges may have complex dependencies with social support in this dataset.
- **Relational Stressor** Cluster: `frd_brk12`, `conf12`, `discrim`, `hea_lit`, `unemp12`, and `rel_end12` form a *looser* cluster focused on social and relational stressors (e.g., friendship breakup, conflicts, and discrimination). Compared to Euclidean clustering, `discrim` and `hea_lit` (health literacy) appear closer to relational stressors here, indicating that non-linear relationships might play a larger role in linking these variables.

6.7.2.2 Summary

In conclusion, mutual information-based clustering provides an alternative perspective that can reveal more intricate associations between variables, especially for those with non-linear relationships. Compared to Euclidean clustering, it shows a similar high-level structure but emphasizes nuanced connections between variables, particularly around social support, employment, and financial stress.

6.8 Conclusions on Precariousness factors

Based on the consistent findings across multiple analyses, we decided to exclude the variables `discrim`, `hea_lit`, `umemp12`, and `rel_end12`, as they do not clearly belong to any specific precariousness factor nor exhibit strong associations with depression (see the correlation table above). Therefore, we propose retaining the following key precariousness factors:

- Employment Precariousness: `emp_stat`, `work_sit`
- Social Precariousness: `soc_freq`, `soc_adq`
- Housing Precariousness: `nb_safe`, `nb_res`, `nb_rent`, `cul_rec`
- Recent Relational Stressors: `frd_brk12`, `conf12`
- Recent Financial Stressors: `fincri12`, `inc_diff`

We construct each precariousness factor by calculating the mean value of the combined variables. Below, we present the updated correlation table for the newly composed factors, along with the corresponding distributions of all variables to be used in the causal discovery analysis.

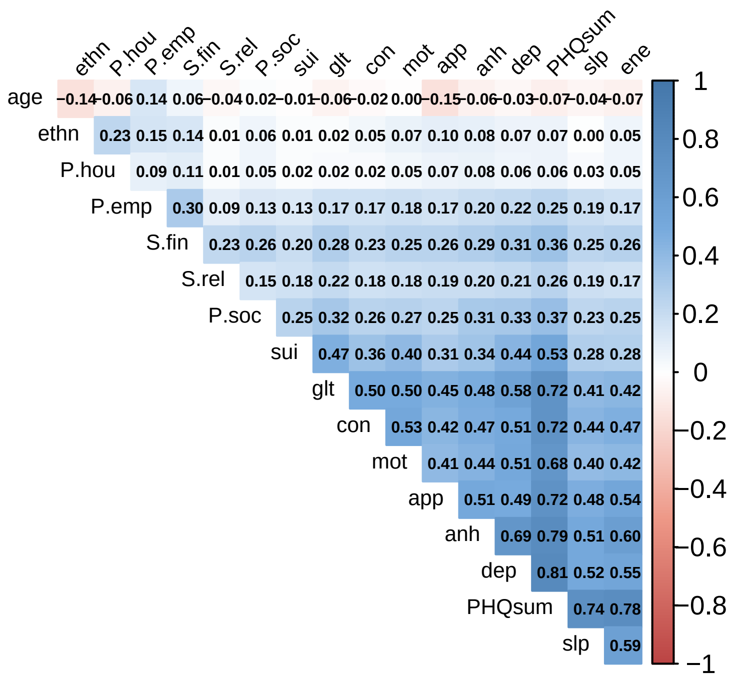

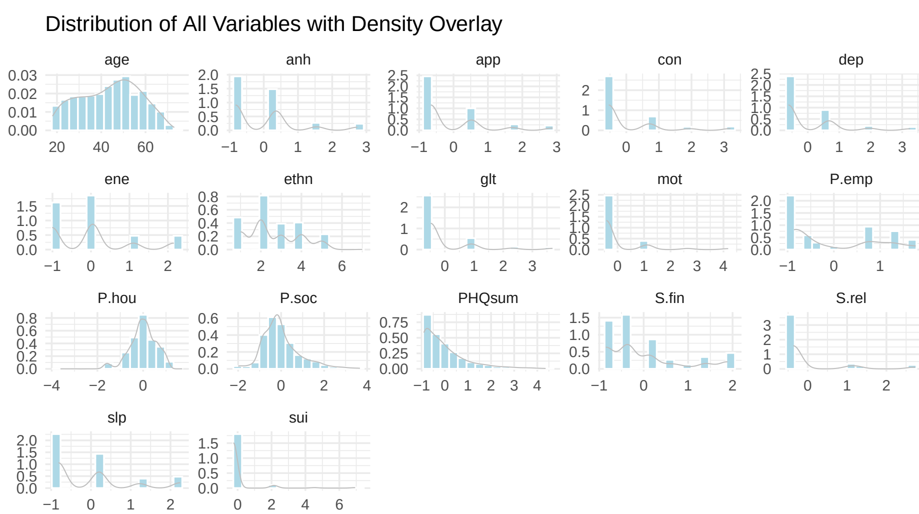

6.9 Results from CCI algorithm

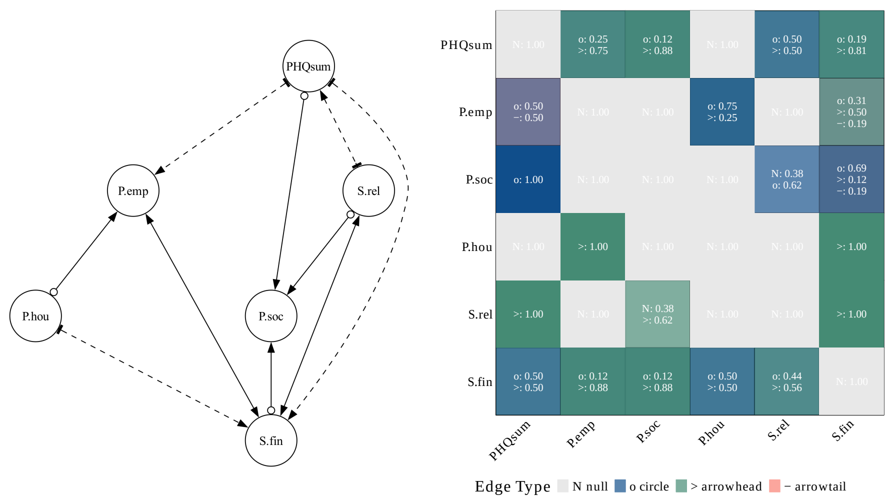

(a) CCI MAAG

(b) Proportion matrix

Figure 10: Resulting graph of precarity factors and depression sum score using CCI and proportion of edge endpoint types.

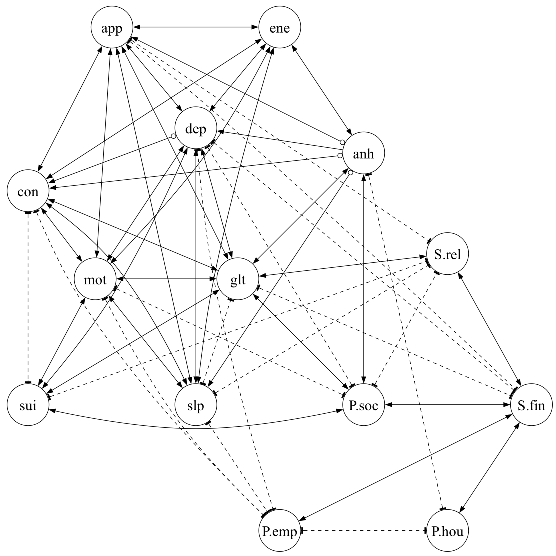

(a) CCI MAAG

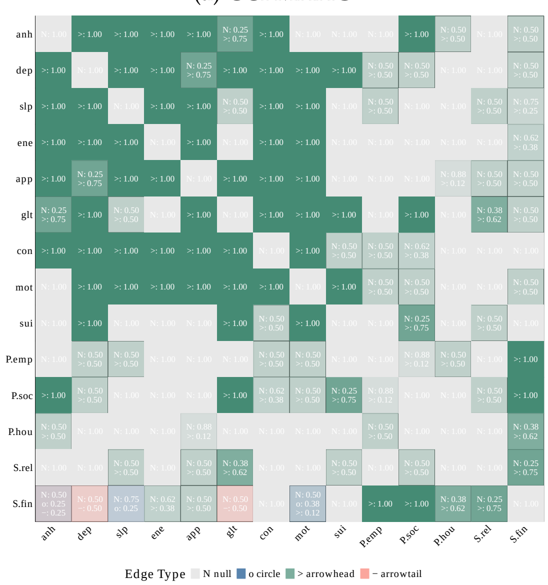

(b) Proportion matrix

Figure 11: Resulting graph of precarity factors and individual depression symptoms using CCI and proportion of edge endpoint types.

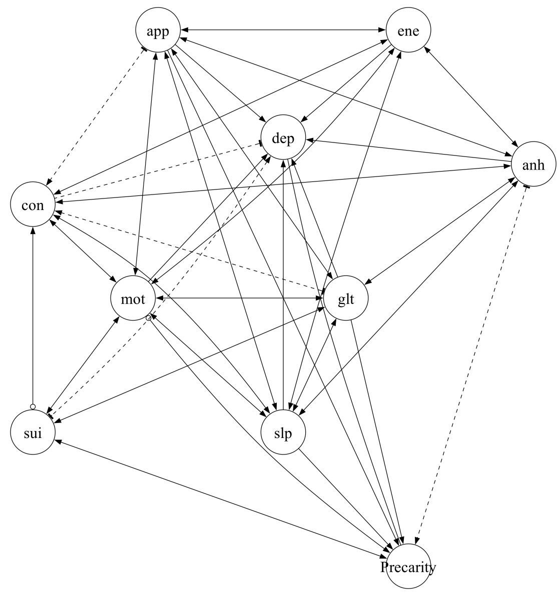

(a) CCI MAAG

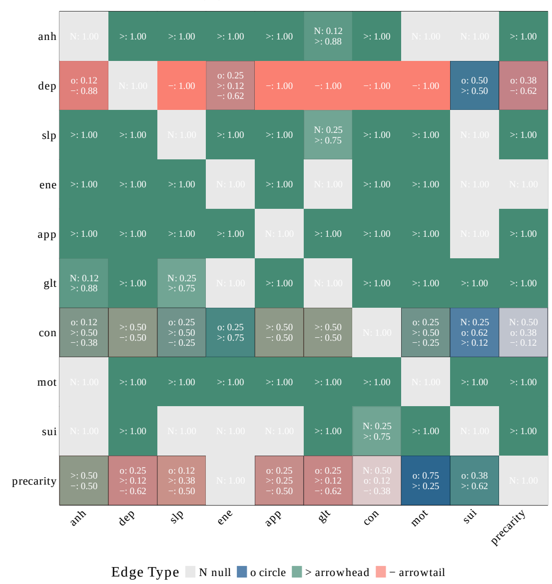

(b) Proportion matrix

Figure 12: Resulting graph of precarity sum score and individual depression symptoms using CCI and proportion of edge endpoint types.

6.10 Results from PC algorithm

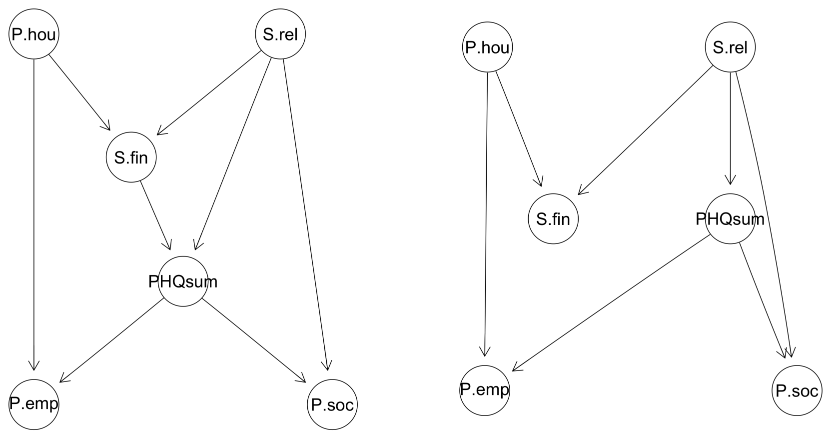

(a) Using both GaussianCI and RCoT

(b) Using only RCoT

Figure 13: Resulting graphs of precarity factors and depression sum score using PC.

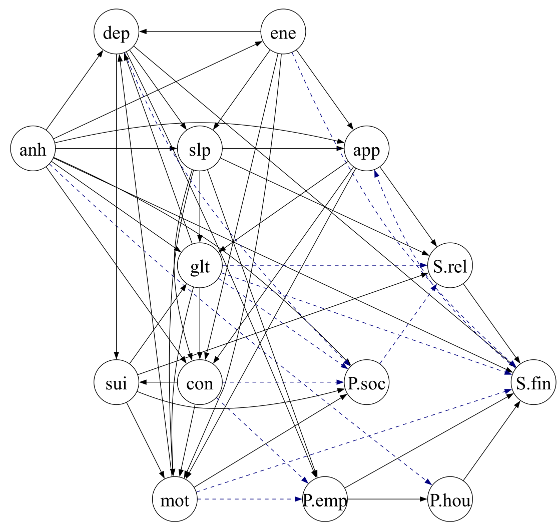

Figure 14: Resulting graphs of precarity factors and individual depression symptoms using PC.

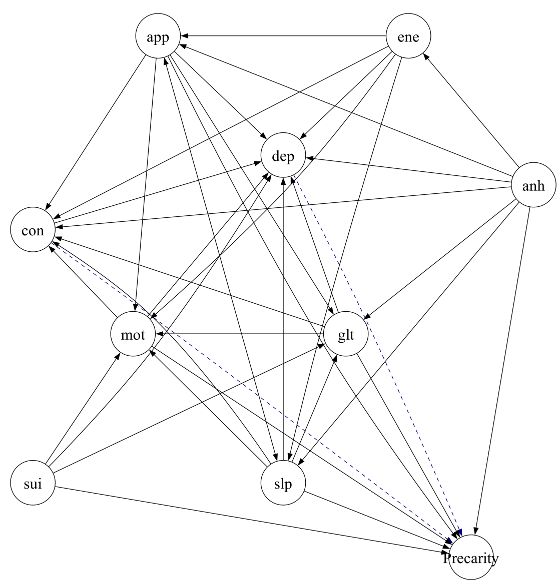

Figure 15: Resulting graphs of precarity sum score and individual depression symptoms using PC.

6.11 Randomized Conditional Independence / Correlation Test (RCIT & RCoT)

RCIT (Randomized Conditional Independence Test) and RCoT (Randomized conditional Correlation Test) are advanced methods for scalable conditional independence (CI) testing, offering computational efficiency while maintaining the accuracy of kernel-based approaches. These methods evaluate conditional independence between two variables X and Y given a third variable Z while addressing computational challenges inherent in kernel-based CI tests. In this section, we provide a high-level overview of RCIT and RCoT based on (Strobl et al., 2019).

6.11.1 Kernel-Based Conditional Independence Testing

Traditional kernel-based CI tests, such as the Kernel Conditional Independence Test (KCIT), compute dependencies using the Hilbert-Schmidt Independence Criterion (HSIC) in reproducing kernel Hilbert spaces (RKHS) (Zhang et al., 2012). KCIT uses the following hypothesis framework:

$$H_0 : X \perp\!\!\!\perp Y \mid Z, \quad H_1 : X \not\perp\!\!\!\perp Y \mid Z.$$

The core quantity in KCIT is the partial cross-covariance operator:

$$\Sigma_{XY \cdot Z} = \Sigma_{XY} - \Sigma_{XZ}\Sigma_{ZZ}^{-1}\Sigma_{ZY},$$

where Σ_{XY} represents the cross-covariance operator between X and Y, and $\Sigma_{XZ}\Sigma_{ZZ}^{-1}\Sigma_{ZY}$ removes the dependence mediated by Z.

The squared Hilbert-Schmidt (HS) norm of $\Sigma_{XY \cdot Z}$ serves as the test statistic:

$$\|\Sigma_{XY \cdot Z}\|_{HS}^2 = 0 \quad \text{if and only if} \quad X \perp\!\!\!\perp Y \mid Z.$$

KCIT estimates residual dependencies using kernel ridge regression:

$$f^*(z) = K_Z(K_Z + \lambda I)^{-1} f(x),$$

where K_Z is the kernel matrix for Z, $f(x)$ is the kernel feature map for X, and λ is the ridge regularization parameter. The residual function for X is:

$$f_{\text{res}}(x) = f(x) - f^*(z) = R_Z f(x),$$

with:

$$R_Z = I - K_Z(K_Z + \lambda I)^{-1}.$$

The kernel matrix for residualized X is:

$$K_{X \cdot Z} = R_Z K_X R_Z,$$

and similarly for Y, $K_{Y \cdot Z} = R_Z K_Y R_Z$.

The test statistic is computed as:

$$T_{XY\cdot Z} = \frac{1}{n^2}\text{tr}(K_{X\cdot Z}K_{Y\cdot Z}),$$

which estimates the Hilbert-Schmidt (HS) norm of the partial cross-covariance operator. To ensure convergence, KCIT scales the statistic by n:

$$S_K = nT_{XY\cdot Z}.$$

The null hypothesis H_0 is rejected if S_K exceeds a threshold determined by permutation or moment-matching-based null distribution (Lindsay et al., 2000).

6.11.2 Random Fourier Features (RFFs)

Kernel-based methods like KCIT face scalability issues, as they involve operations on $n \times n$ kernel matrices, which scale quadratically with the sample size n. RCIT and RCoT overcome this bottleneck using *Random Fourier Features (RFFs)* to approximate kernel operations efficiently.

6.11.2.1 Bochner's Theorem

Bochner's theorem provides the foundation for RFFs, stating that any continuous shift-invariant kernel $k(x, y)$ can be expressed as:

$$k(x, y) = \int_{\mathbb{R}^p} e^{i\omega^\top (x-y)}\, dP_\omega,$$

where P_ω is the spectral distribution of the kernel. For the widely used RBF kernel:

$$k(x, y) = \exp\left(-\frac{\|x - y\|^2}{2\sigma^2}\right),$$

P_ω follows a Gaussian distribution: $\omega \sim \mathcal{N}(0, \sigma^2 I)$.

6.11.2.2 RFF Approximation

Using Monte Carlo sampling, the kernel function is approximated as:

$$k(x, y) \approx \phi(x)^\top \phi(y),$$

where $\phi(x)$ is the random Fourier feature mapping:

$$\phi(x) = \sqrt{\frac{2}{D}}\cos(W^\top x + b),$$

with $W \sim \mathcal{N}(0, \sigma^2 I)$ and $b \sim \text{Uniform}(0, 2\pi)$. Here, D is the number of Fourier features, which balances computational efficiency and approximation accuracy.

6.11.3 Differences Between RCIT and RCoT

RCIT and RCoT differ in their test statistics, computational efficiency, and practical performance, which makes them suited for different scenarios in causal discovery. RCIT evaluates the Hilbert-Schmidt norm of the full partial cross-covariance operator, providing a general test for conditional independence but at a higher computational cost. RCoT simplifies the process by using the Frobenius norm of a finite-dimensional residualized cross-covariance matrix, significantly reducing complexity and improving scalability.

These distinctions are particularly important for large-scale datasets, where RCoT's computational efficiency makes it a practical choice for high-dimensional causal discovery tasks.

6.11.3.1 RCIT: Randomized Conditional Independence Test

RCIT tests full conditional independence by examining the squared Hilbert-Schmidt (HS) norm of the partial cross-covariance operator $\Sigma_{XY \cdot Z}$:

$$S_K = nT_{XY \cdot Z} = \frac{1}{n}\text{tr}(K_{X \cdot Z} K_{Y \cdot Z}),$$

where $T_{XY \cdot Z}$ is an empirical estimate of $\|\Sigma_{XY \cdot Z}\|_{HS}^2$. The null and alternative hypotheses are:

$$H_0 : \|\Sigma_{XY \cdot Z}\|_{HS}^2 = 0, \quad H_1 : \|\Sigma_{XY \cdot Z}\|_{HS}^2 > 0.$$

RCIT is a general test for conditional independence but becomes computationally demanding as the size of Z increases, due to the high-dimensional kernel operations required.

6.11.3.2 RCoT: Randomized Conditional Correlation Test

RCoT simplifies the testing process by using a finite-dimensional partial cross-covariance matrix, avoiding full HS norm calculations. Instead, it uses the Frobenius norm of the residualized cross-covariance matrix:

$$S' = n\|C_{AB \cdot C}\|_F^2,$$

where $C_{AB \cdot C}$ represents the residualized cross-covariance matrix. The hypotheses are:

$$H_0 : \|C_{AB \cdot C}\|_F^2 = 0, \quad H_1 : \|C_{AB \cdot C}\|_F^2 > 0.$$

RCoT is computationally efficient and well-suited for large conditioning sets ($|Z| \geq 4$). Its simplicity enables robust calibration of the null distribution and improved scalability for high-dimensional data.

Acknowledgements

The HELIUS study is conducted by the Amsterdam University Medical Centers, location AMC and the Public Health Service of Amsterdam. Both organisations provided core support for HELIUS. The HELIUS study is also funded by the Dutch Heart Foundation, the Netherlands Organization for Health Research and Development (ZonMw), the European Union (FP-7), and the European Fund for the Integration of non-EU immigrants (EIF). We are most grateful to the participants of the HELIUS study and the management team, research nurses, interviewers, research assistants and other staff who have taken part in gathering the data of this study.